

Fabrication of plasma transient density structures and its application to high-field plasma devices

Szu-yuan Chen

Institute of Atomic and Molecular Sciences, Academia Sinica, Taipei, Taiwan

Department of Physics, National Central University, Jhong-Li, Taiwan



collaborating principal investigators

Jyhpyng Wang

Institute of Atomic and Molecular Sciences, Academia Sinica

Jiunn-Yuan Lin

Department of Physics, National Chung Cheng University

experimental team

C.-T. Hsieh , C.-L. Chang, T.-Y. Chien, Y.-C. Ho,
M.-C. Chou, P.-H. Lin, H.-E. Tsai, Y.-F. Xiao, H.-H. Chu,
C.-H. Pai, M.-W. Lin, C.-C. Kuo, K.-H. Lee, Y.-M. Chen

Outline

- **Fabrication of plasma density structures by laser machining**

- Fabrication by a transverse laser beam
- Fabrication by a longitudinal laser beam
- Patterning of the machining beam by liquid-crystal spatial light modulator and adaptive feedback optimization of products

- **Tomography of high-field physics in a gas jet**

- Tomography of self-injected laser wakefield electron accelerator
- Tomography of optical-field-ionization collisional-excitation x-ray laser in a cluster jet
- Tomography of high-harmonic generation in a gas or cluster jet

- **High-field plasma devices**

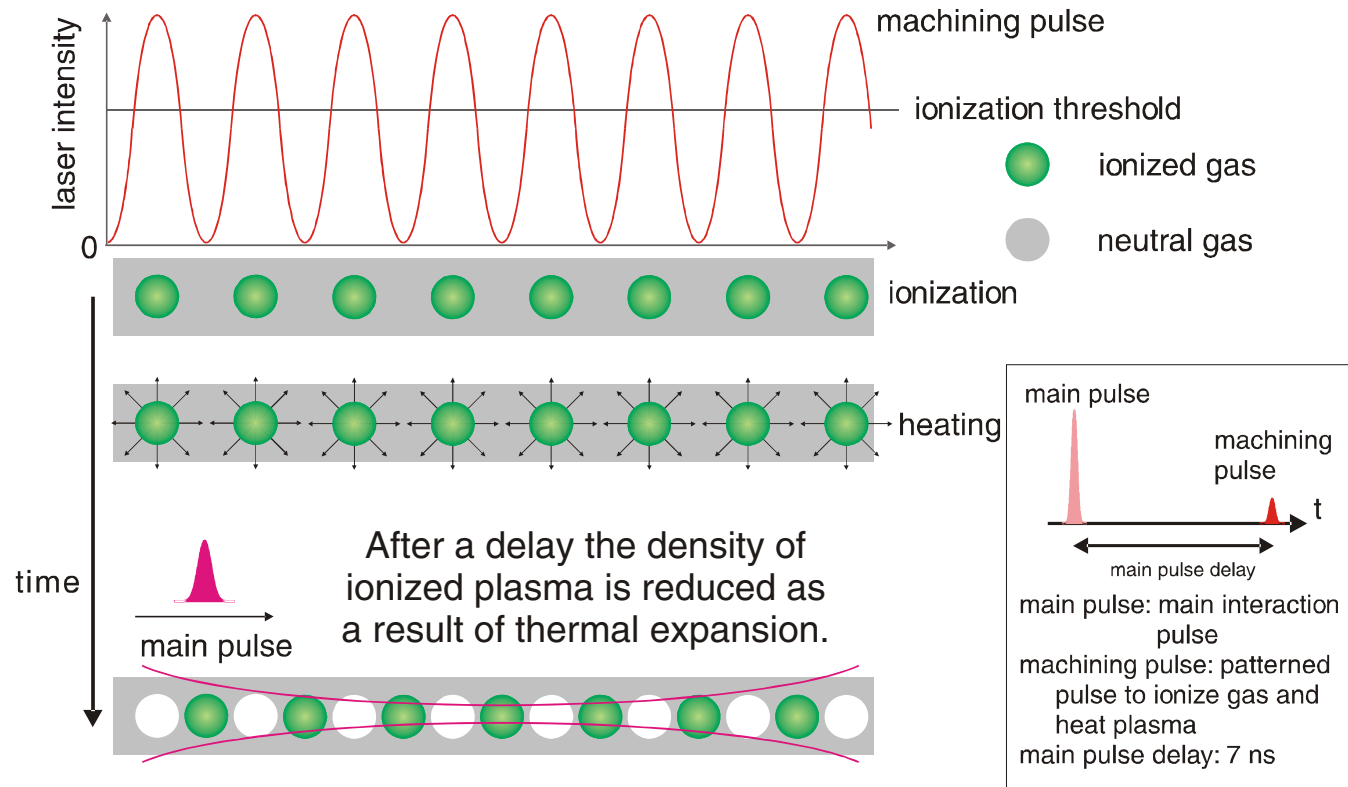
- Electron injector
- Quasi-phase matching of harmonic generation and particle acceleration
- Electron wiggler for x-ray production

- **Conclusion**

Fabrication of plasma density structures by laser machining

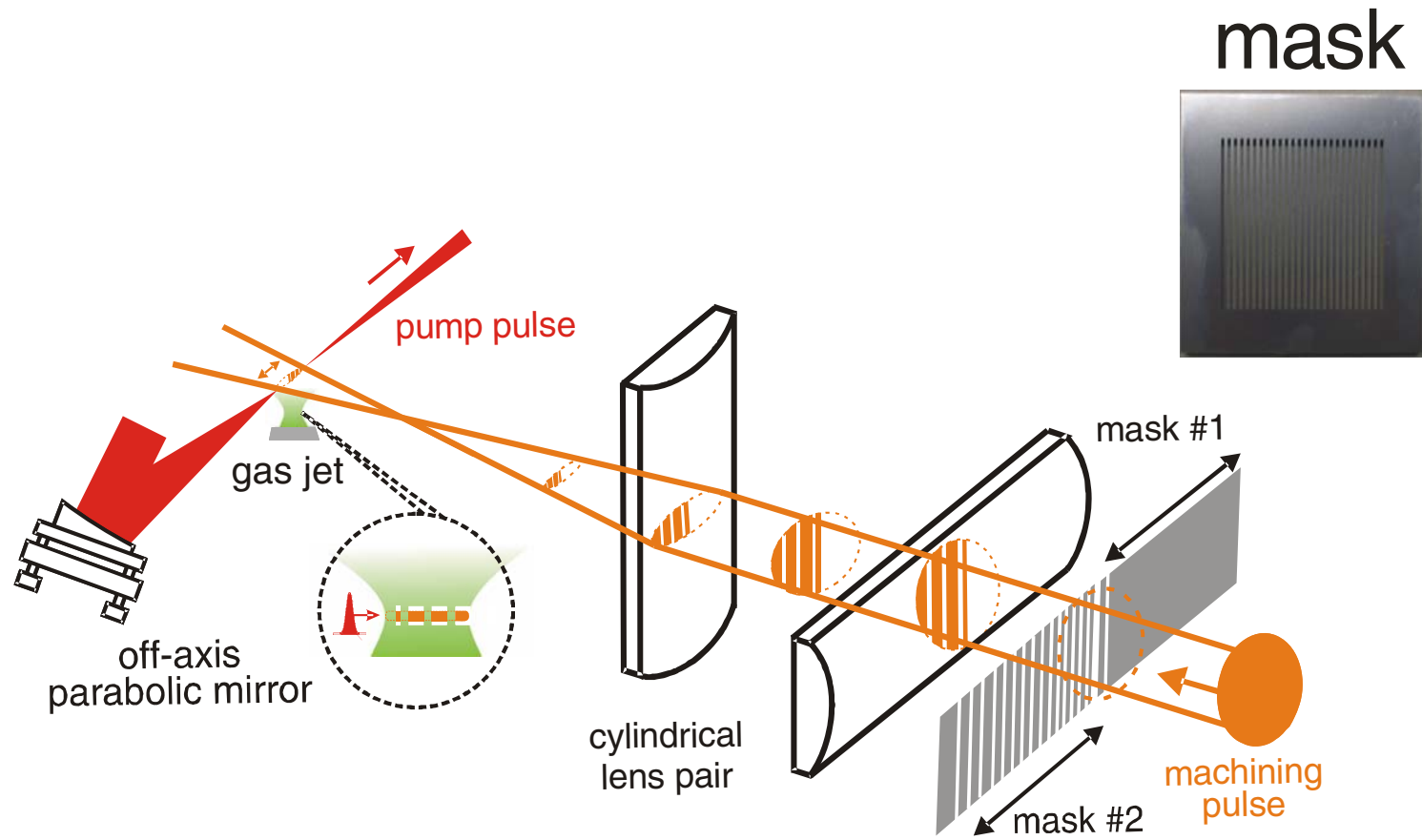
Fabrication by a transverse laser beam

Principle for fabrication of spatial structures in gas/plasma



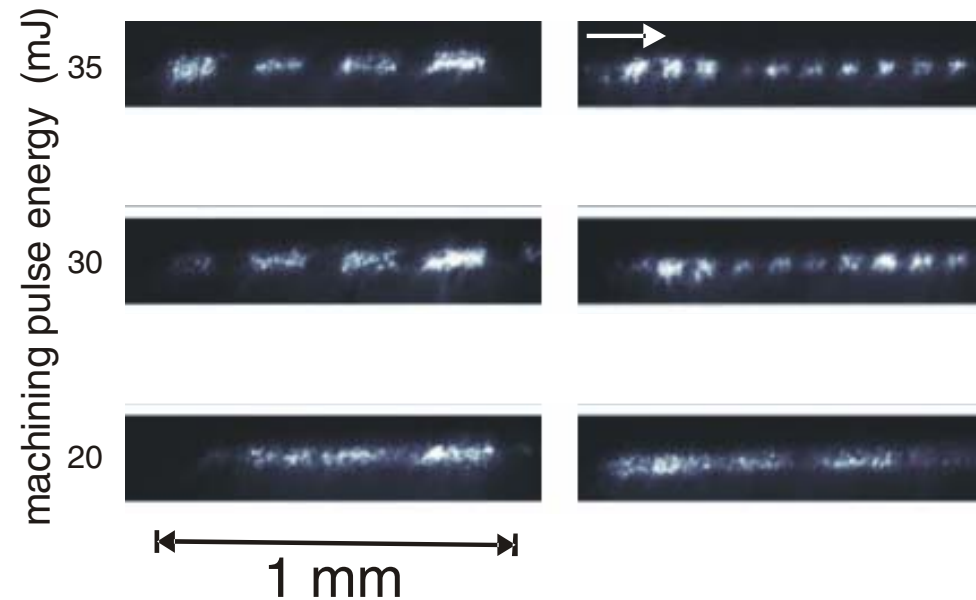
- ⦿ The machining pulse plays both the roles of ionizing the gas through optical-field ionization and heating the plasma by above-threshold-ionization (ATI) heating and inverse bremsstrahlung heating.

Experimental setup



Gas structures of 250 μm and 100 μm period

H_2 $2.5 \times 10^{19} \text{ cm}^{-3}$

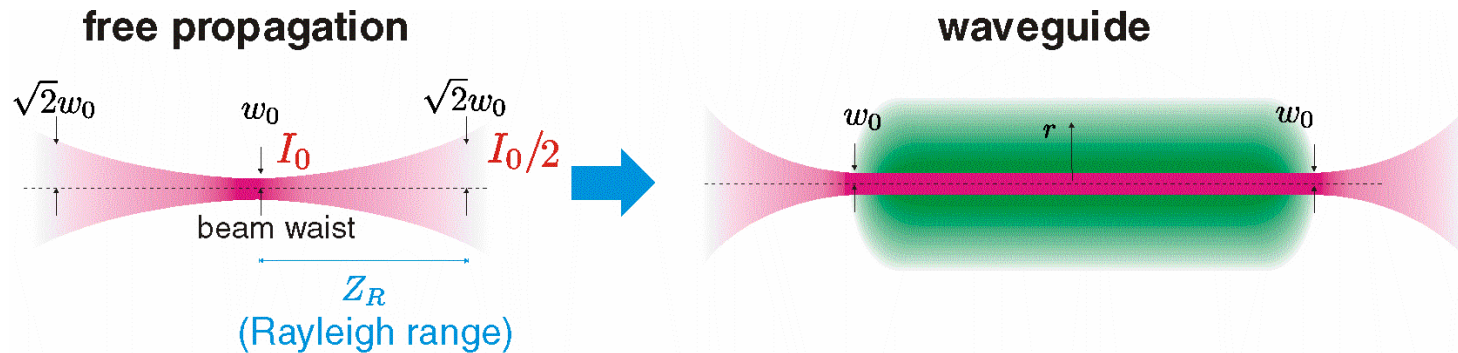


- Sharp periodic structures with a boundary scale length approaching $10 \mu\text{m}$ was produced in hydrogen when the machining pulse energy was larger than 20 mJ.

Fabrication of plasma density structures by laser machining

Fabrication by a longitudinal laser beam

Purpose of a plasma waveguide



$$Z_R = \pi w_0^2 / \lambda \quad \text{Rayleigh range}$$

$$I_0 = \frac{2E}{\tau \pi w_0^2} \quad \text{peak intensity}$$

E : pulse energy

τ : pulse duration

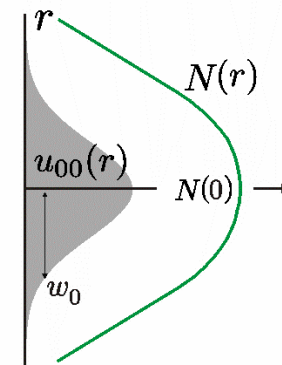
w_0 : beam waist

refractive index depends quadratically on r

$$N(r) = N(0) \left[1 - \frac{r^2}{2h^2} \right]$$

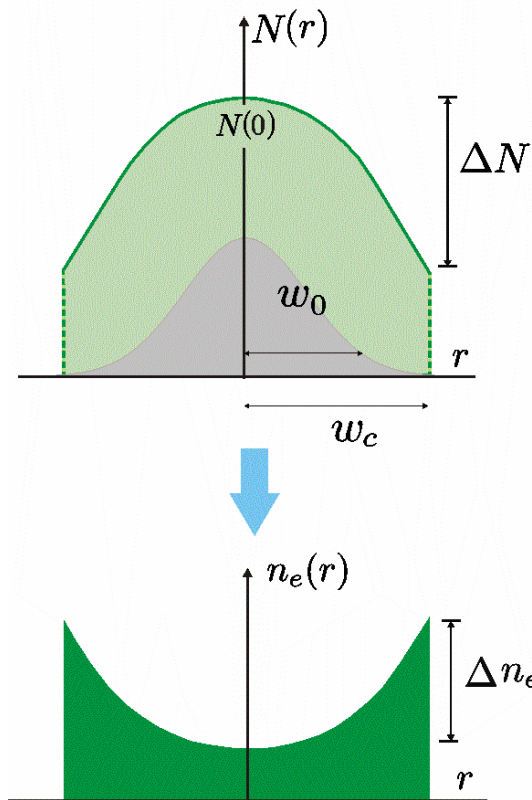
relation between h and w_0

$$w_0^2 = \frac{2h}{k_0}$$



- ⇒ For a focused Gaussian beam, the axial intensity is inversely proportional to the Rayleigh range. However, by using a plasma waveguide, a laser beam can propagate a long distance while maintaining high intensity.

Guiding condition in a plasma waveguide



difference of refractive index

$$\Delta N = \frac{w_c^2}{2h^2} = \frac{w_c^2 \lambda^2}{2\pi^2 w_0^4}$$

refractive index of plasma

$$N = \sqrt{1 - \frac{4\pi e n_e}{m_e \omega^2}}$$

n_e : electron density

m_e : electron mass

ω : plasma frequency

the minimum guiding condition

$$w_c > w_0$$

$$\Delta N > \frac{\lambda^2}{2\pi^2 w_0^2}$$

$$\Delta n_e > \frac{m_e c^2}{e\pi w_0^2}$$

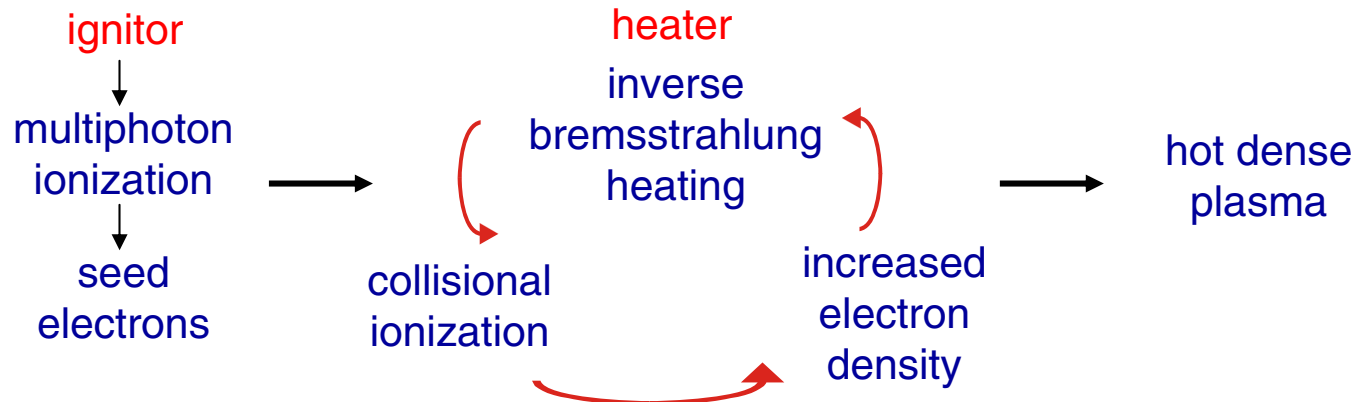
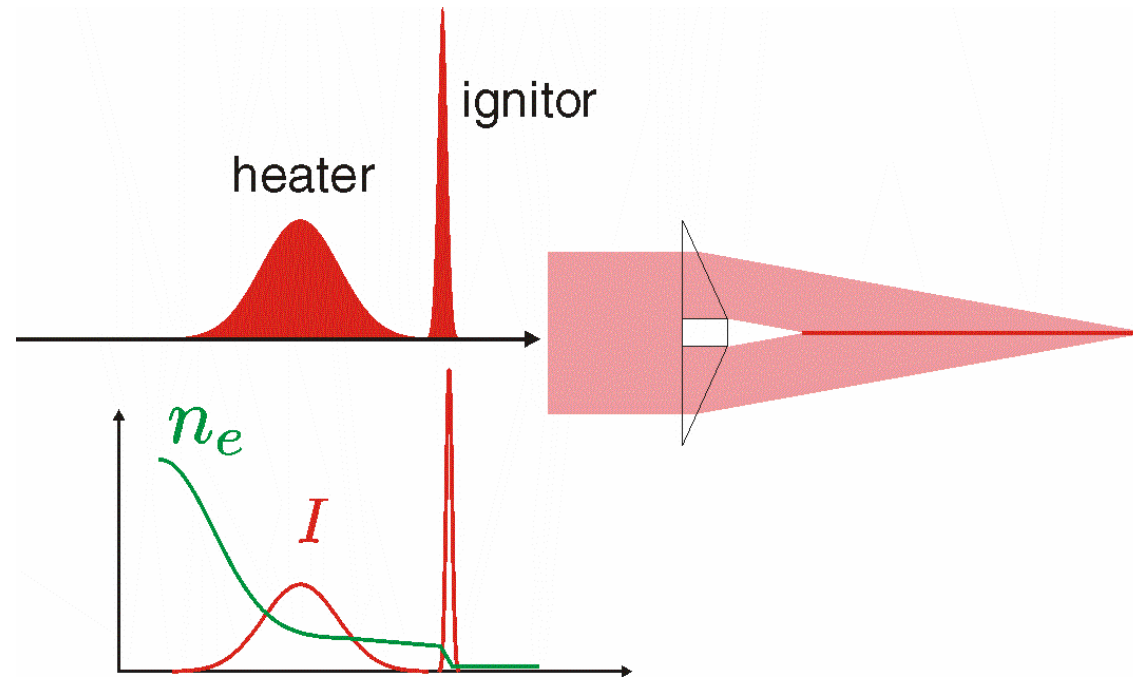
w_c : waveguide radius

Δn_e : difference of
electron density

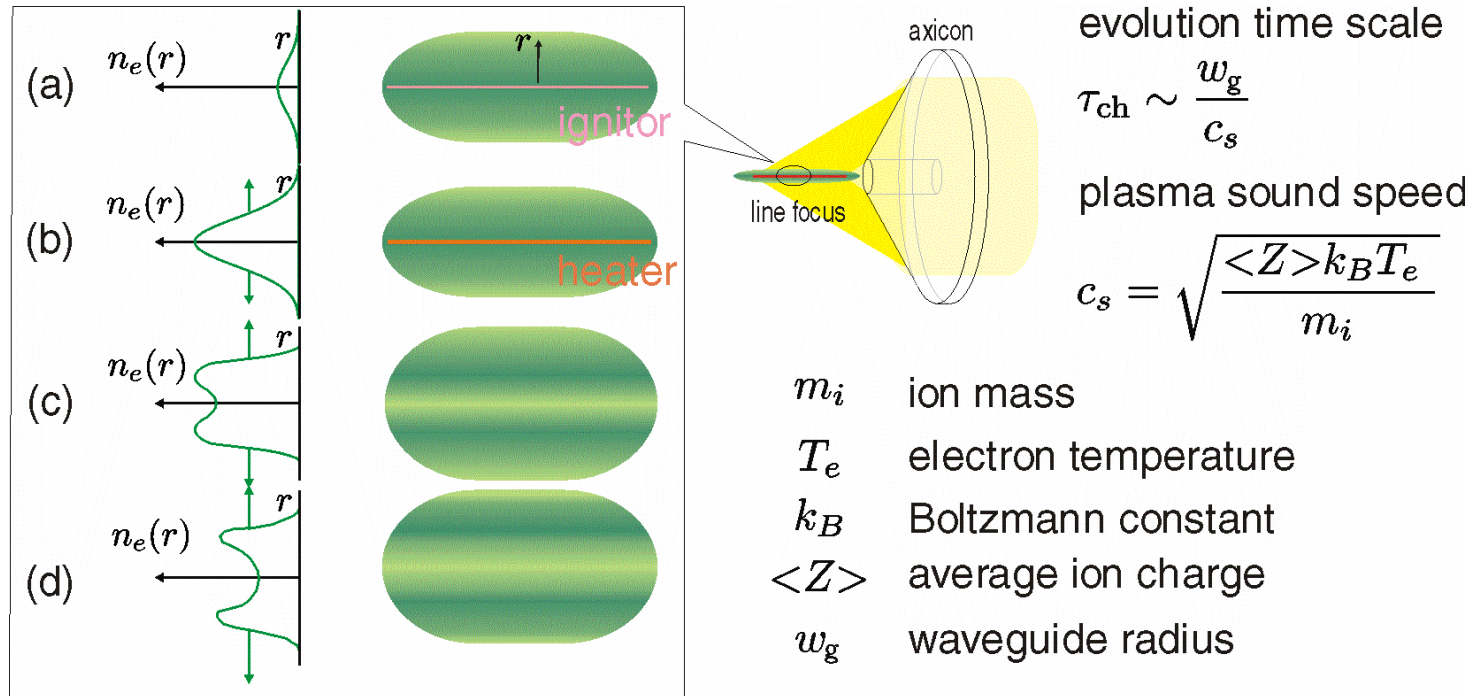
w_0 : beam waist

⇒ The required density difference is independent of guided laser wavelength from infrared to soft x-ray.

Seeded avalanche breakdown

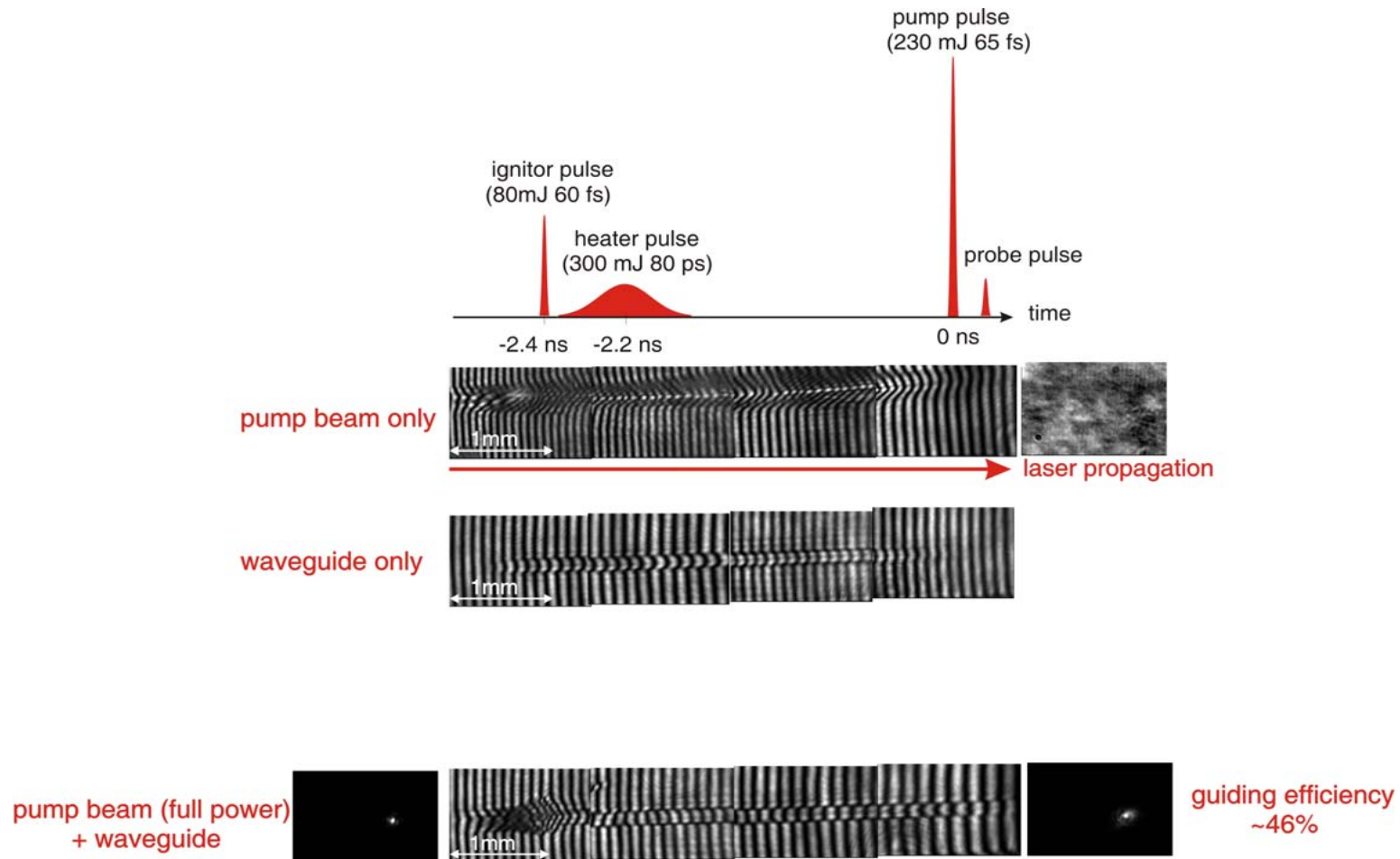


Formation of a plasma waveguide driven by a laser line focus



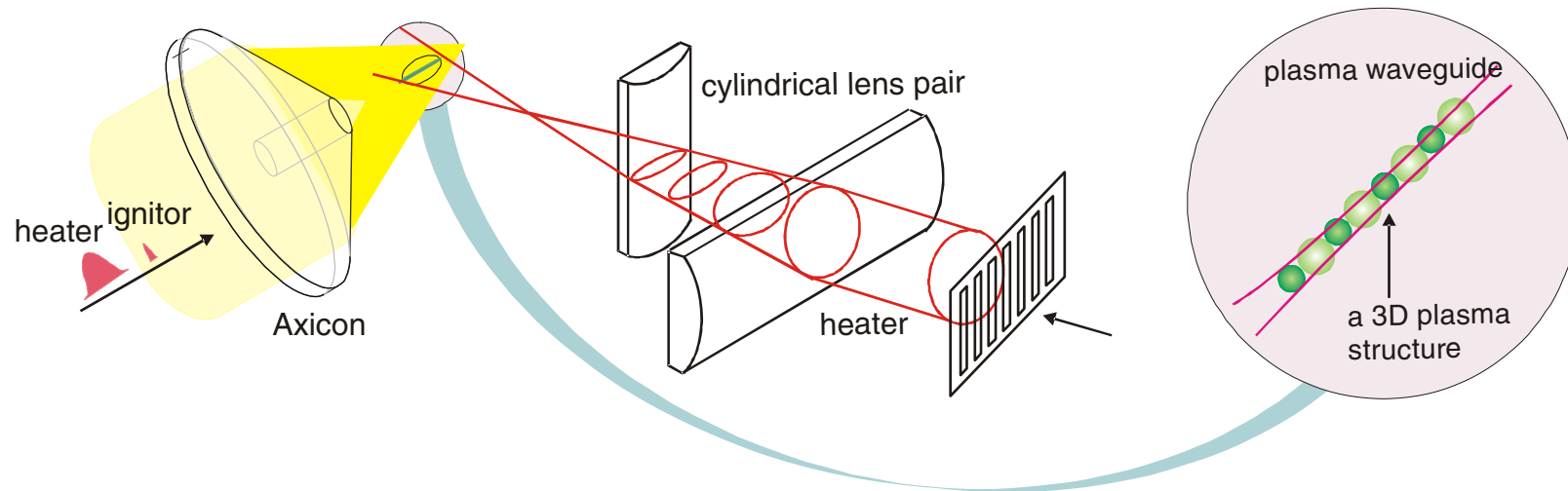
- The shock wave expansion causes plasma density buildup at the periphery, forming a plasma waveguide.

Guiding of the pump pulse by a plasma waveguide in a 5-mm hydrogen gas jet



- ⇒ The plasma waveguide is completed upon the arrival of the pump pulse, so more than 46% of the pump pulse energy is guided.

Corrugated plasma waveguide

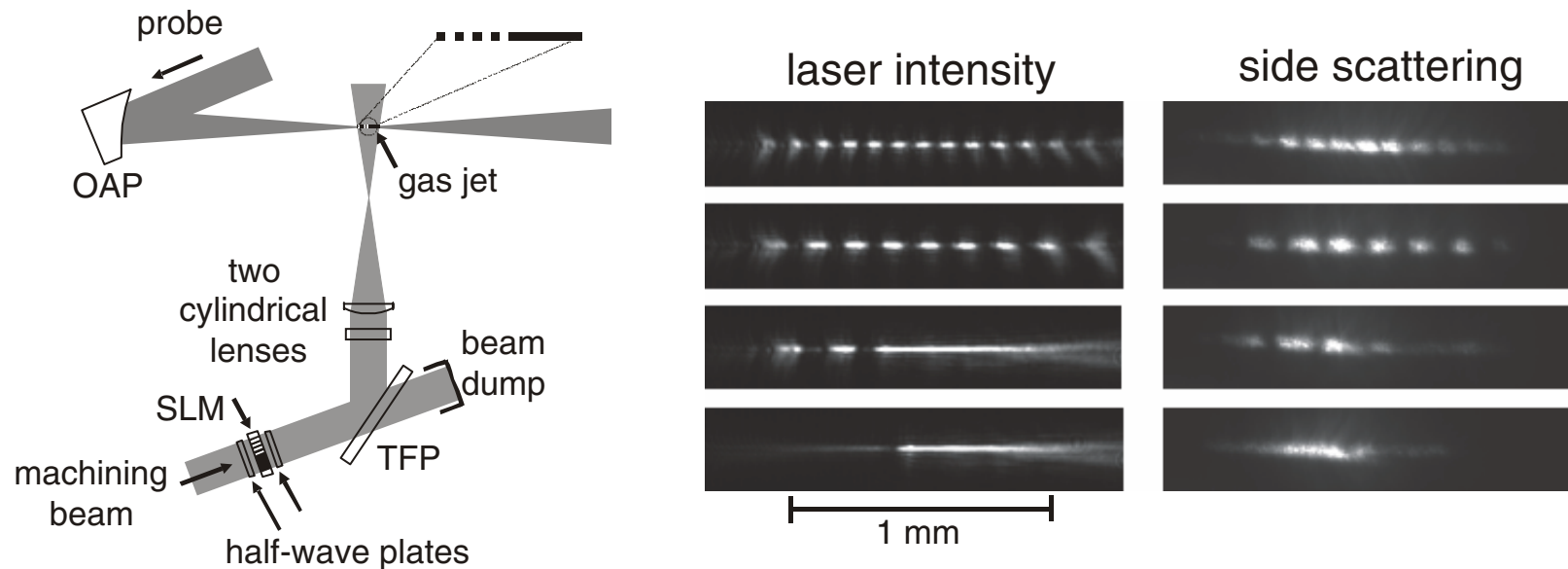


- A corrugated plasma waveguide can be applied to quasi-phase-matched relativistic harmonic generation, wakefield electron accelerator, etc.

Fabrication of plasma density structures by laser machining

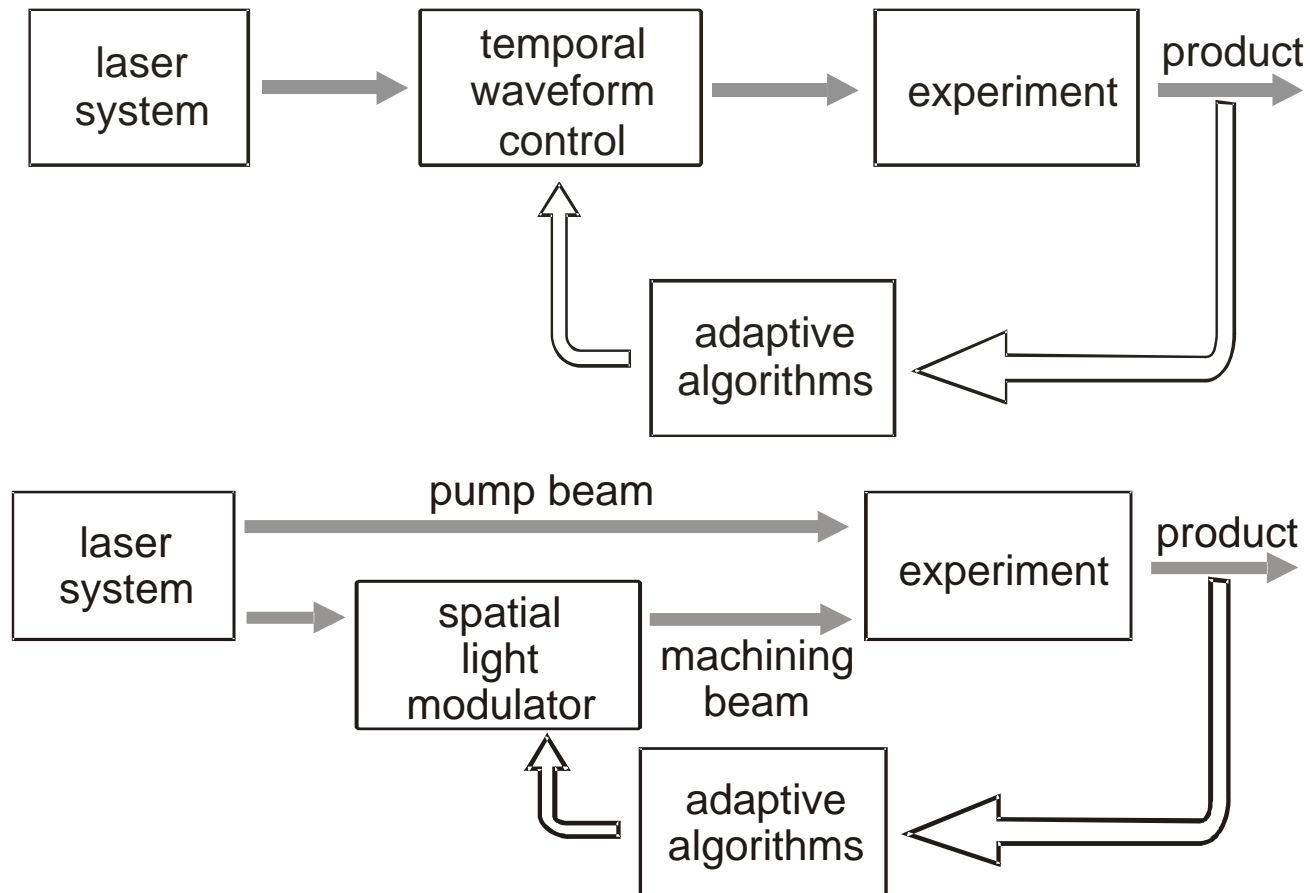
Patterning of the machining beam by liquid-crystal spatial light modulator and adaptive feedback optimization of products

Programmable fabrication of longitudinal density structures



- By replacing the patterned mask with a liquid-crystal spatial light modulator (SLM), programmable fabrication of longitudinal density structures can be achieved.
- The SLM also allows fine adjustment of the intensity at each pixel to compensate for effects such as diffraction and B-integral or to obtain wide-range uniformity, which cannot be achieved by using hard masks.

Adaptive feedback optimization of products



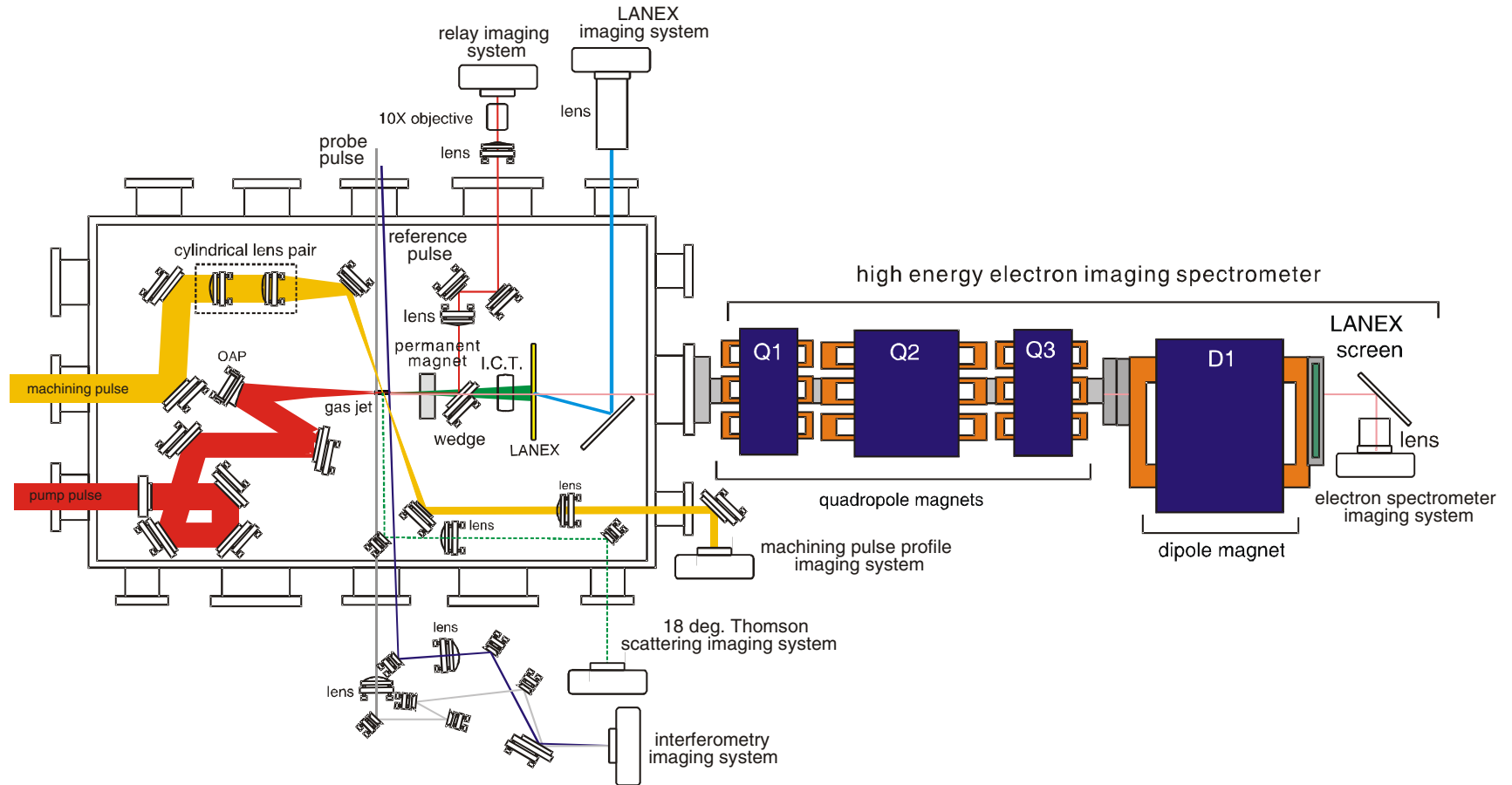
- In a way similar to adaptive feedback optimization of laser temporal waveform for quantum coherent control, this technique enables adaptive feedback optimization of gas/plasma spatial structure for enhancing the characteristics of products of various high-field plasma photonic devices.

Tomography of high-field physics in a gas jet

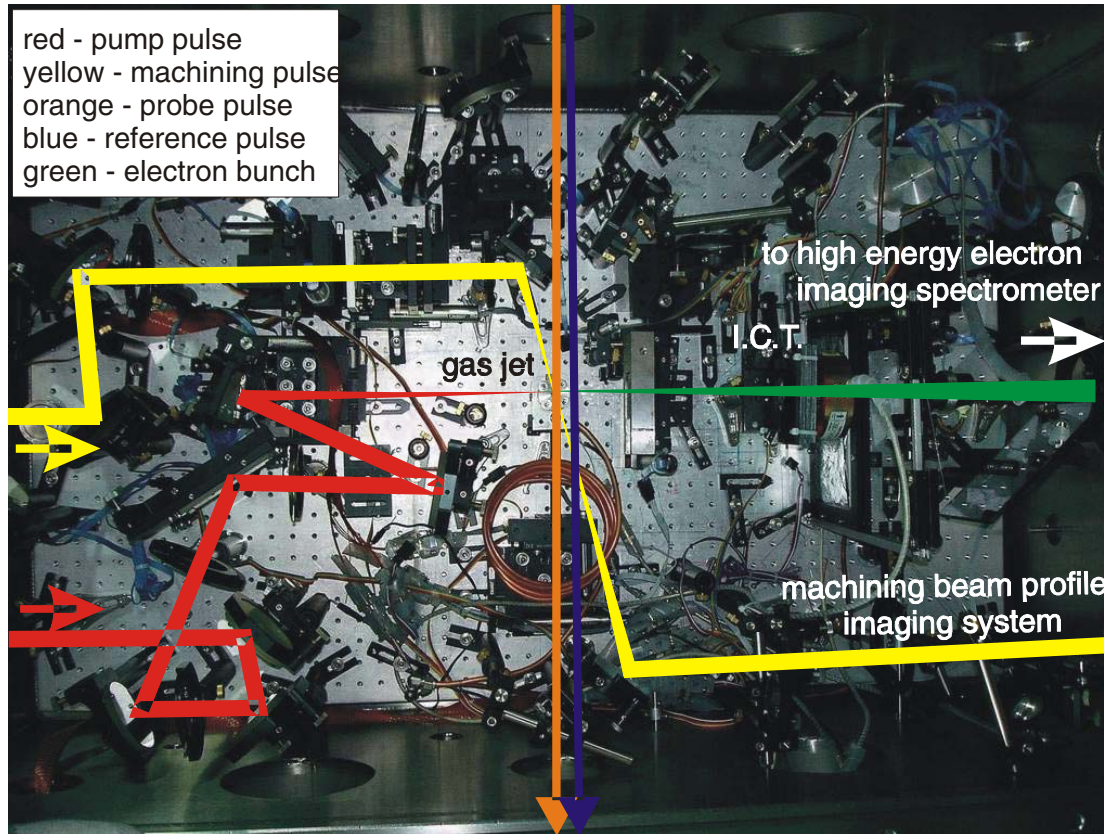
Tomography of self-injected laser wakefield electron
accelerator

Physical Review Letters **96**, 095001 (2006)

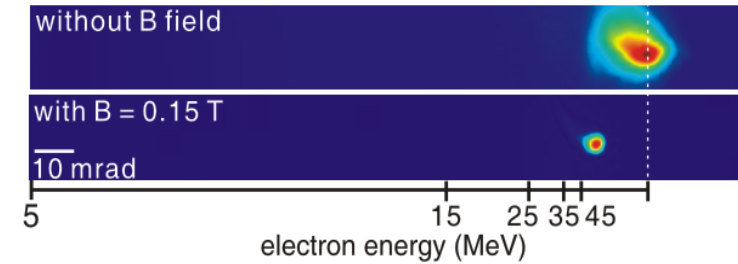
Experimental setup



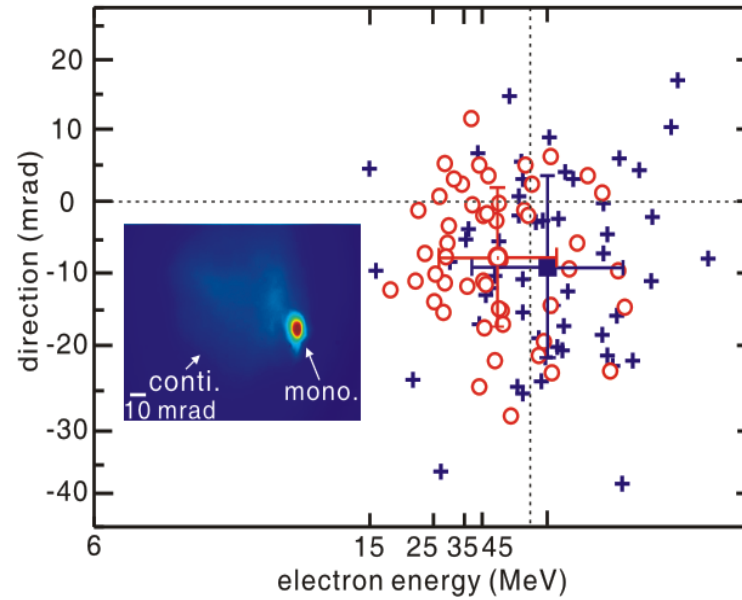
Experimental setup



Monoenergetic electron beam and beam pointing fluctuation

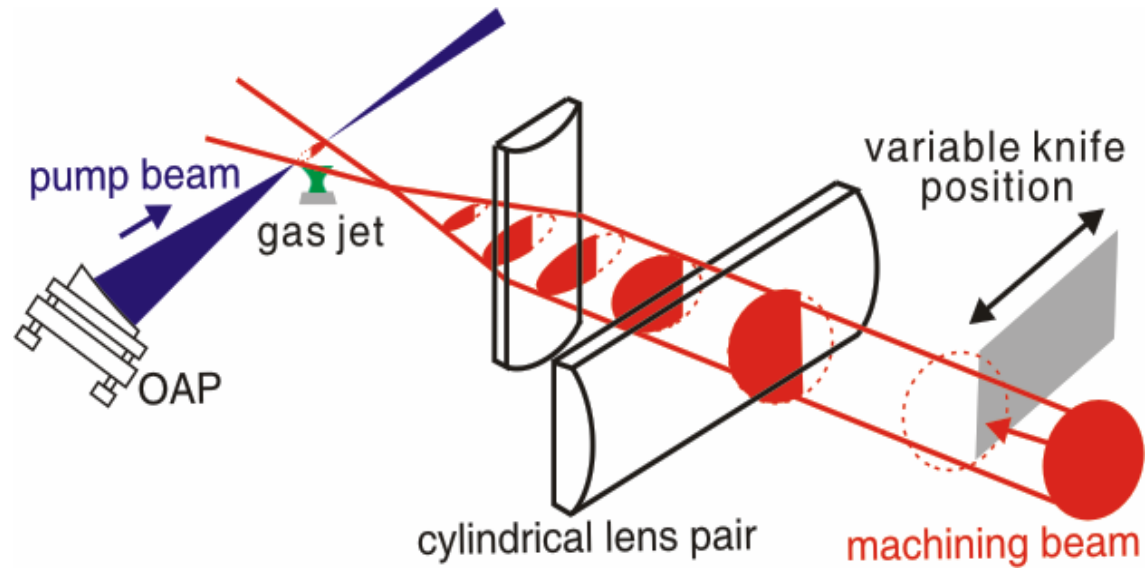


230 mJ, 45 fs
 $4 \times 10^{19} \text{ cm}^{-3}$ plasma density



- Because the beam pointing fluctuation reaches 20 mrad in standard deviation and thus it can lead to misjudgement of the energy of the monoenergetic electron beam and overestimate of the electron energy fluctuation.

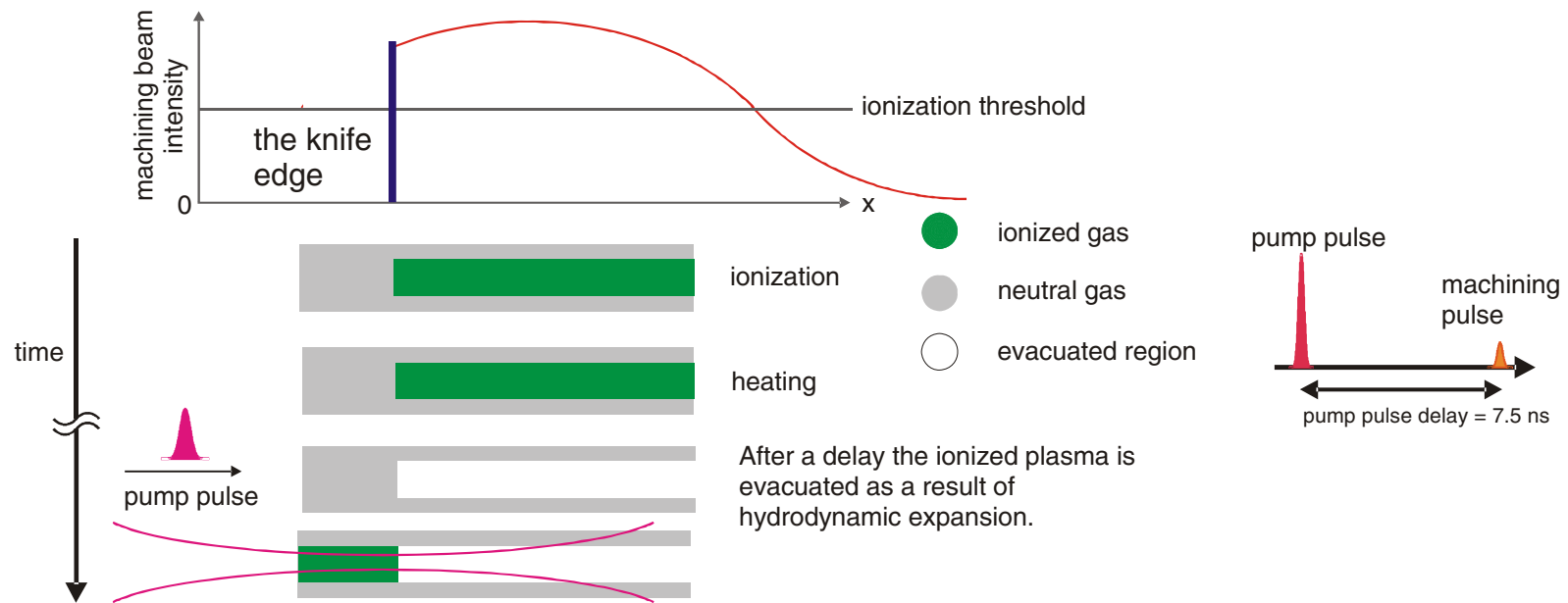
Experimental setup



laser parameters:

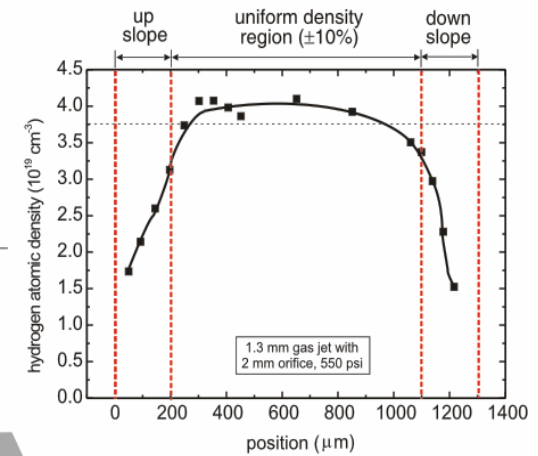
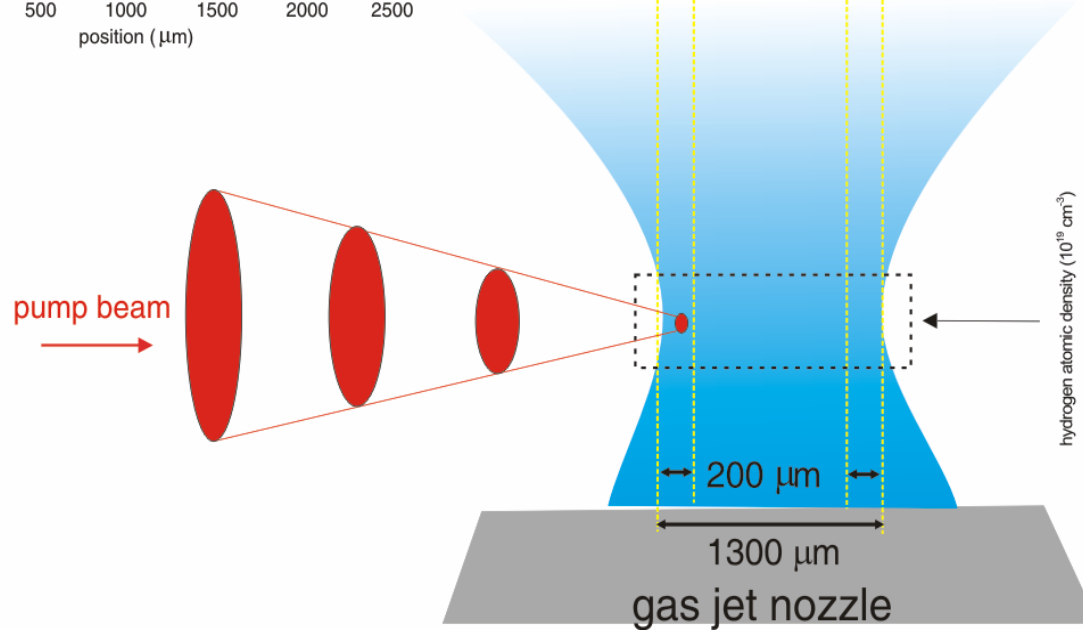
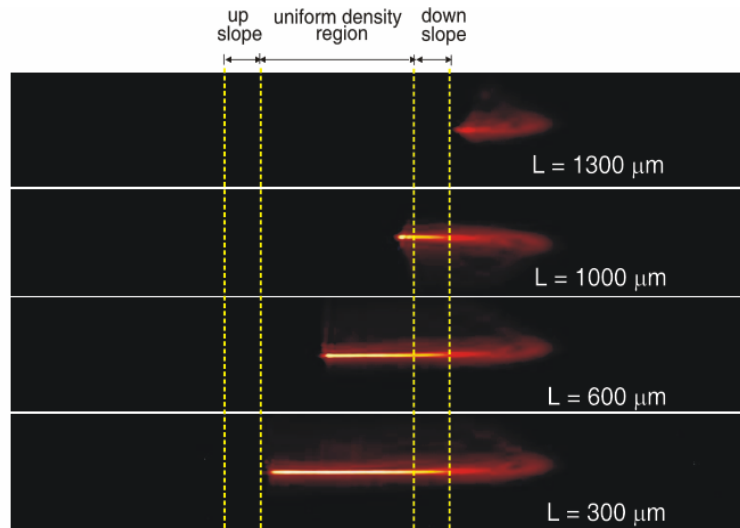
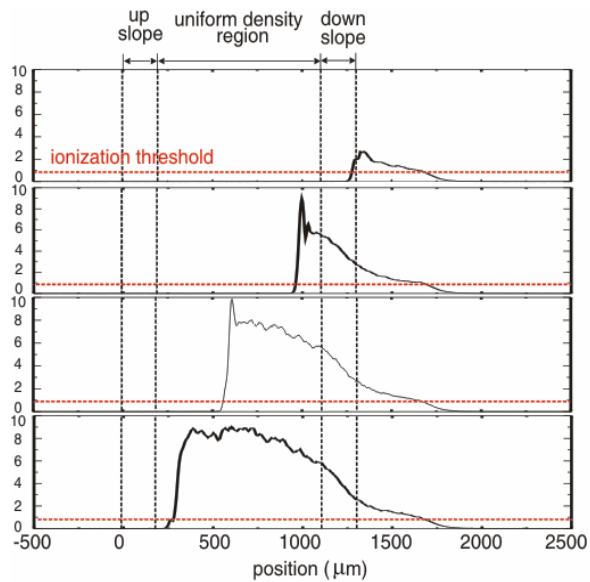
	pump beam	machining beam
energy	230 mJ	60 mJ
pulse duration (FWHM)	45 fs	45 fs
beam size	40 mm	40 mm
focal spot (FWHM)	10 μm	20 μm x 1.3 mm

Principle of tomography using laser machining

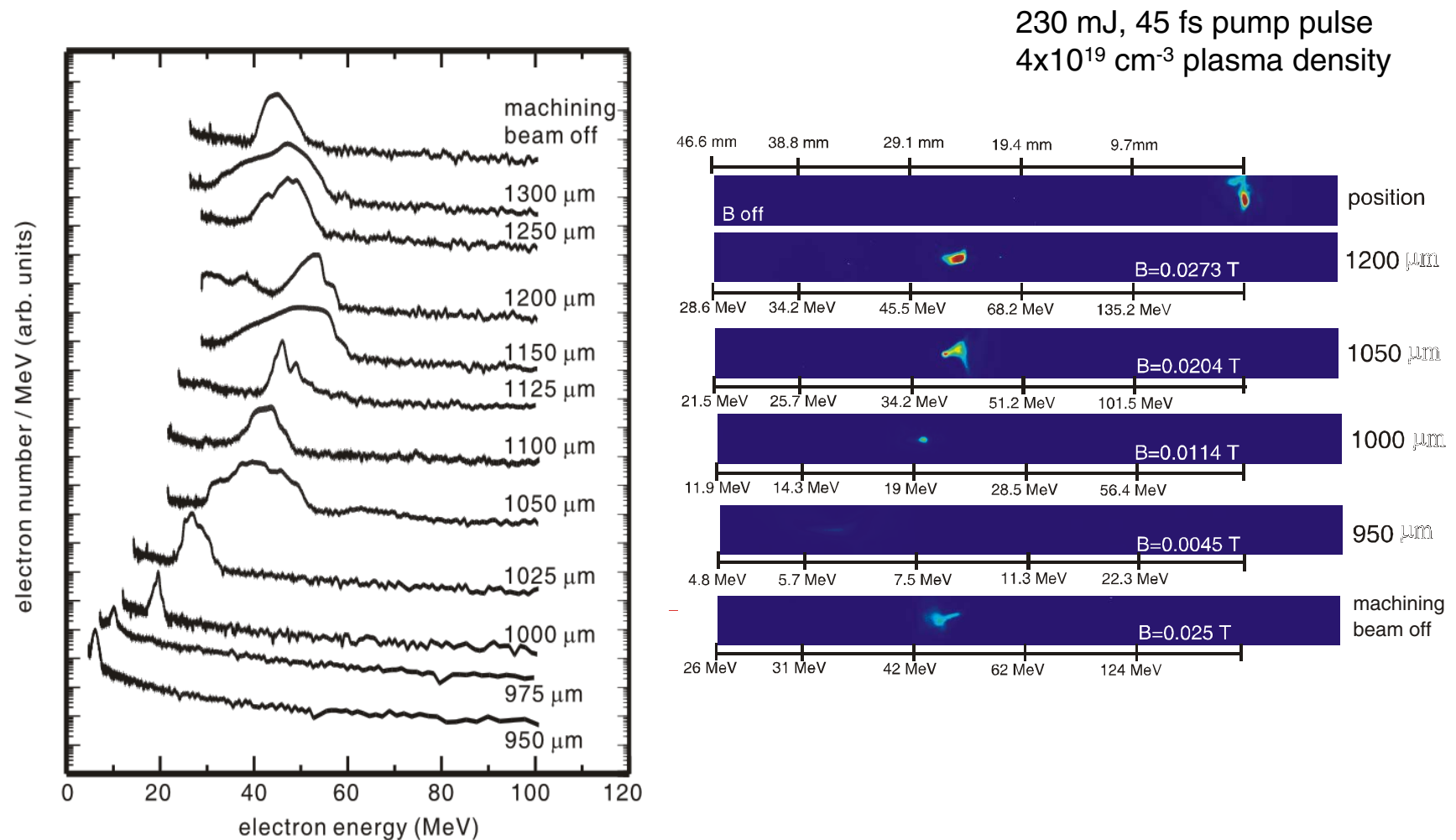


(a) The laser intensity inside the gas jet is set to be larger than the intensity threshold of optical-field ionization. (b) Atoms illuminated by the machining beam are ionized. (c) Heating of the plasma by the machining beam leads to plasma hydrodynamic expansion. (d) After several nanoseconds the region ionized by the machining beam is evacuated. (e) The characteristics of the electron beam accelerated by the plasma wave driven by the longitudinal pump pulse at the position corresponding to that of the knife edge is measured.

Intensity profile of the machining beam on the propagation axis of the pump beam



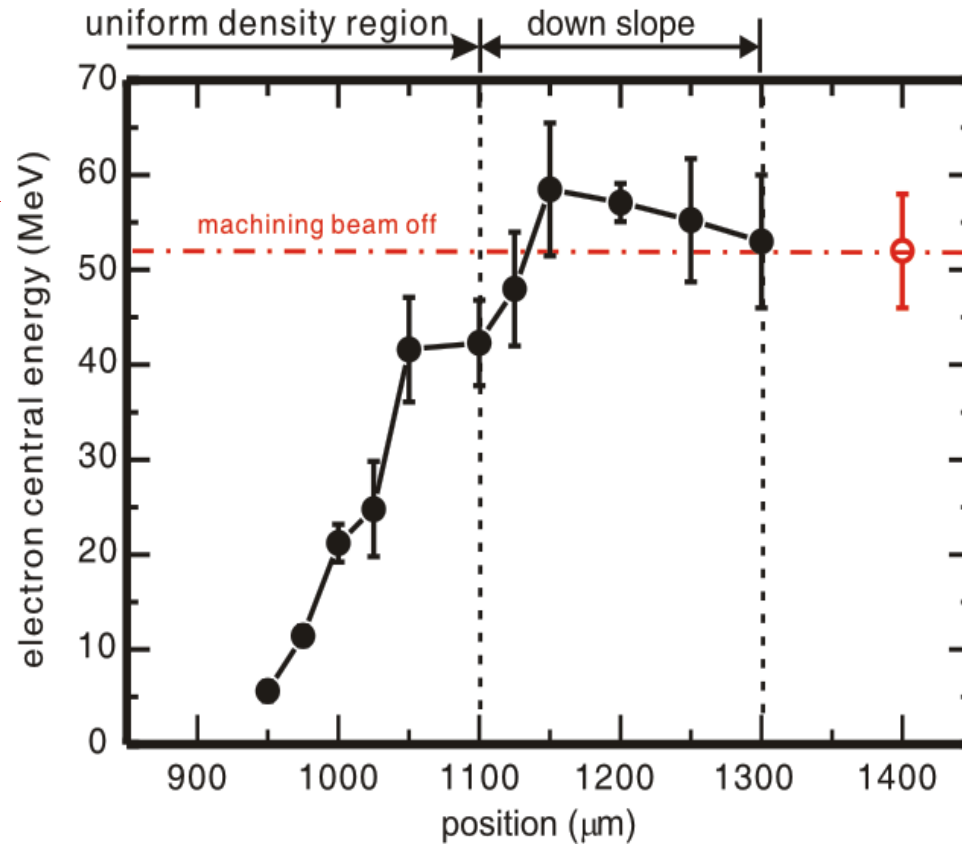
Electron energy spectra at various positions in the gas jet



- Although the resolution of energy spread was still limited by the spot size of the electron beam on the LANEX screen, it can be seen that the monoenergetic electron beam has already a finite energy spread right after its injection and stays so during the acceleration.

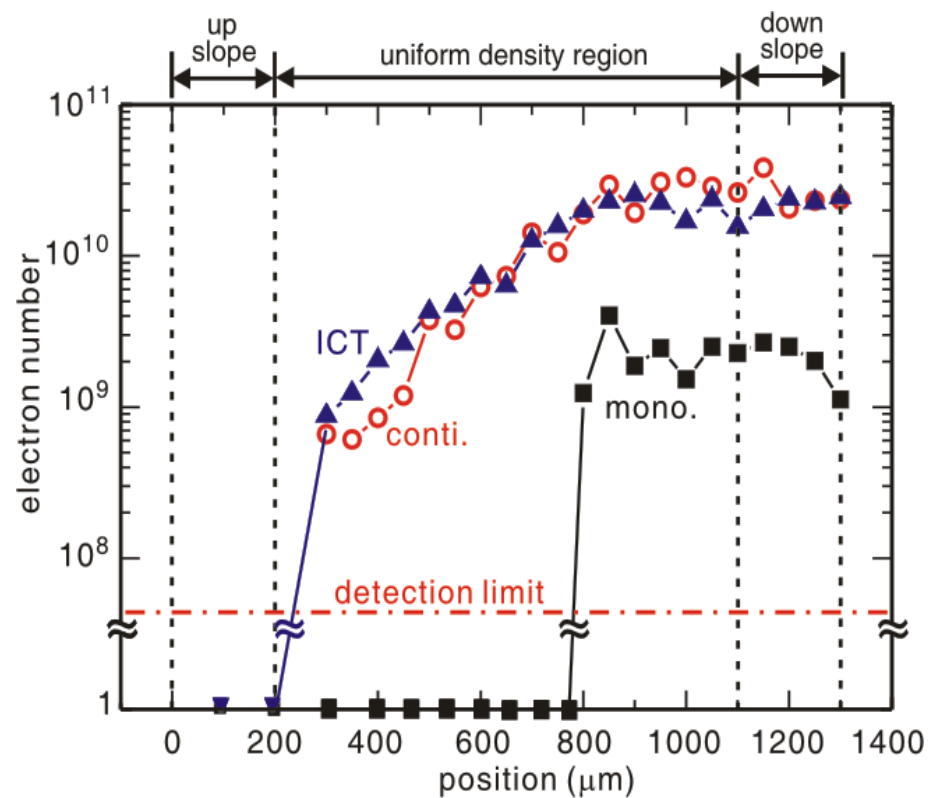
Central energy of the monoenergetic electron beam at various positions

230 mJ, 45 fs pump pulse
 $4 \times 10^{19} \text{ cm}^{-3}$ plasma density



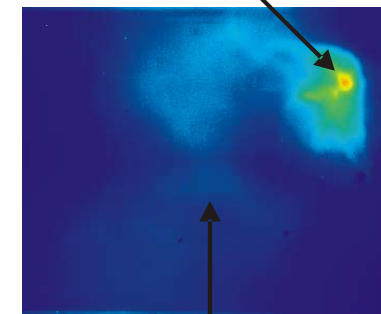
- The energy of the monoenergetic electron beam increases roughly linearly from 5 MeV at 950- μm position to 55 MeV at 1150- μm position, corresponding to an acceleration gradient of $\sim 2.5 \text{ GeV/cm}$.

Numbers of monoenergetic electrons and continuum electrons at various positions



230 mJ, 45 fs pump pulse
 $4 \times 10^{19} \text{ cm}^{-3}$ plasma density

monoenergetic electrons



10 mrad

continuum electrons

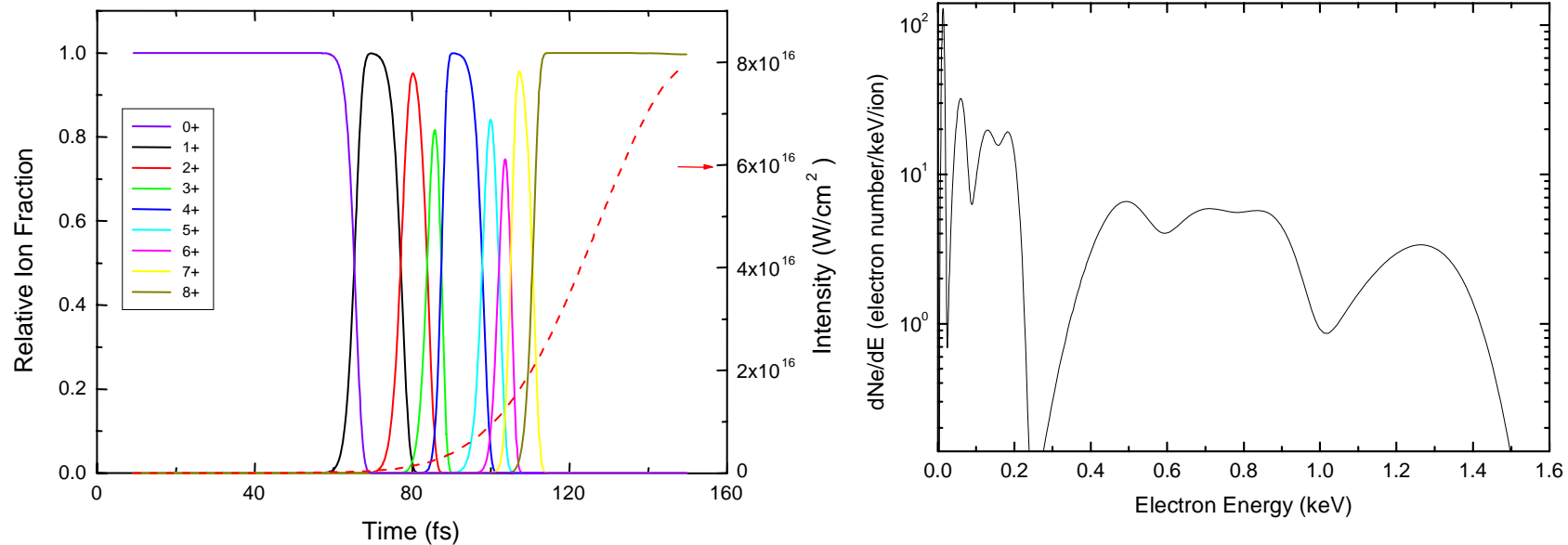
- ⇒ The injection of continuum electrons starts at 300- μm position and occurs continuously until 800- μm position.
- ⇒ The monoenergetic electrons are injected at 800- μm position and no further injection occurs afterwards.
- ⇒ After the injection of the monoenergetic electrons the increase of number of continuum electrons ceases, in agreement with damping of plasma wave by beam loading.

Tomography of high-field physics in a gas jet

Tomography of optical-field-ionization collisional-excitation x-ray laser in a cluster jet

submitted to Physical Review A

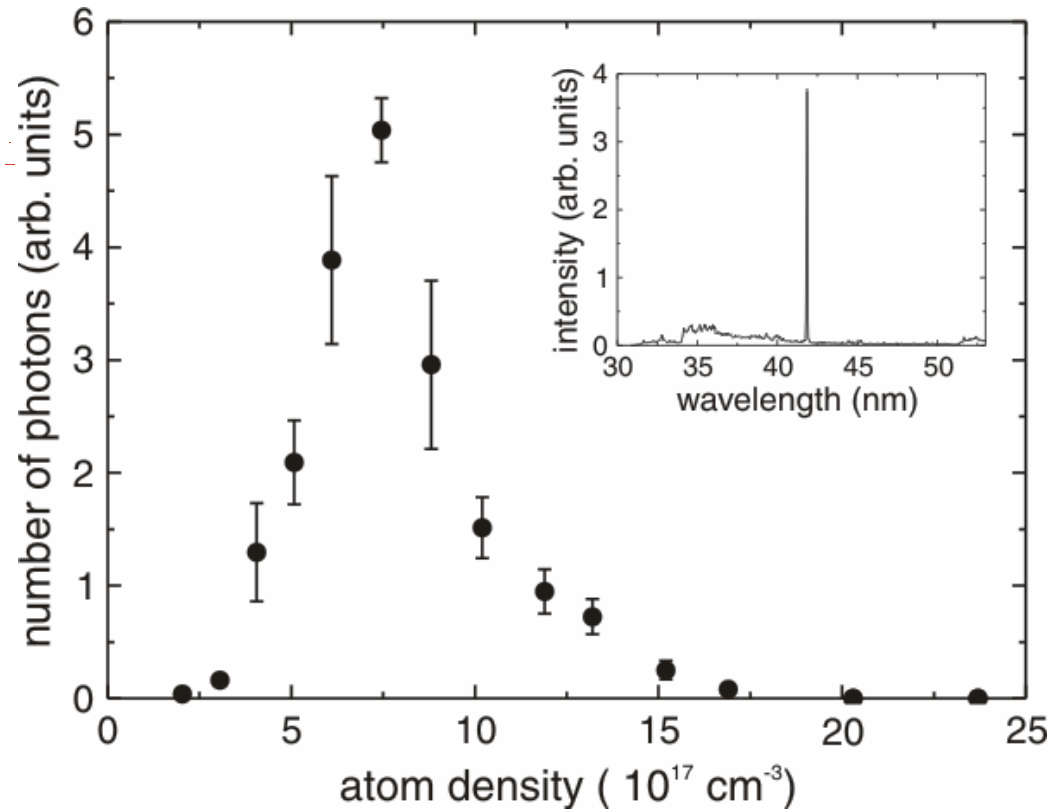
Principle of optical-field-ionization collisional-excitation x-ray laser



- When a laser pulse with appropriate laser intensity is incident into a gas jet, atoms in the jet can be ionized to specific ion species through optical-field-ionization. At the same time the electrons gain energy from above-threshold-ionization heating and collide with the lasing ions to achieve population inversion between the excited states.

X-ray lasing intensity vs. atom density

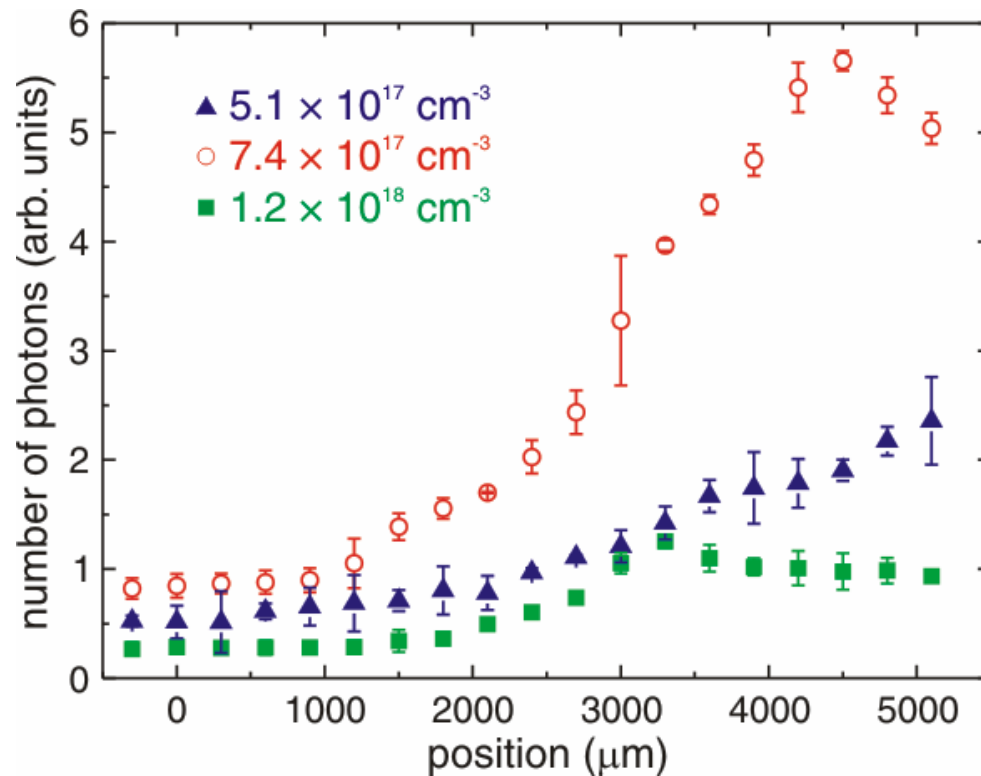
45 fs, 210 mJ, polarization ellipticity = 0.65
focus position at 2500 μm



- An optimal atom density for maximum lasing intensity was found at $7.4 \times 10^{17} \text{ cm}^{-3}$. Its presence was believed to result from the trade-off between increased gain and decreased gain length resulting from ionization-induced refraction with increasing atom density.

Growth of x-ray lasing intensity with pump propagation for various atom densities

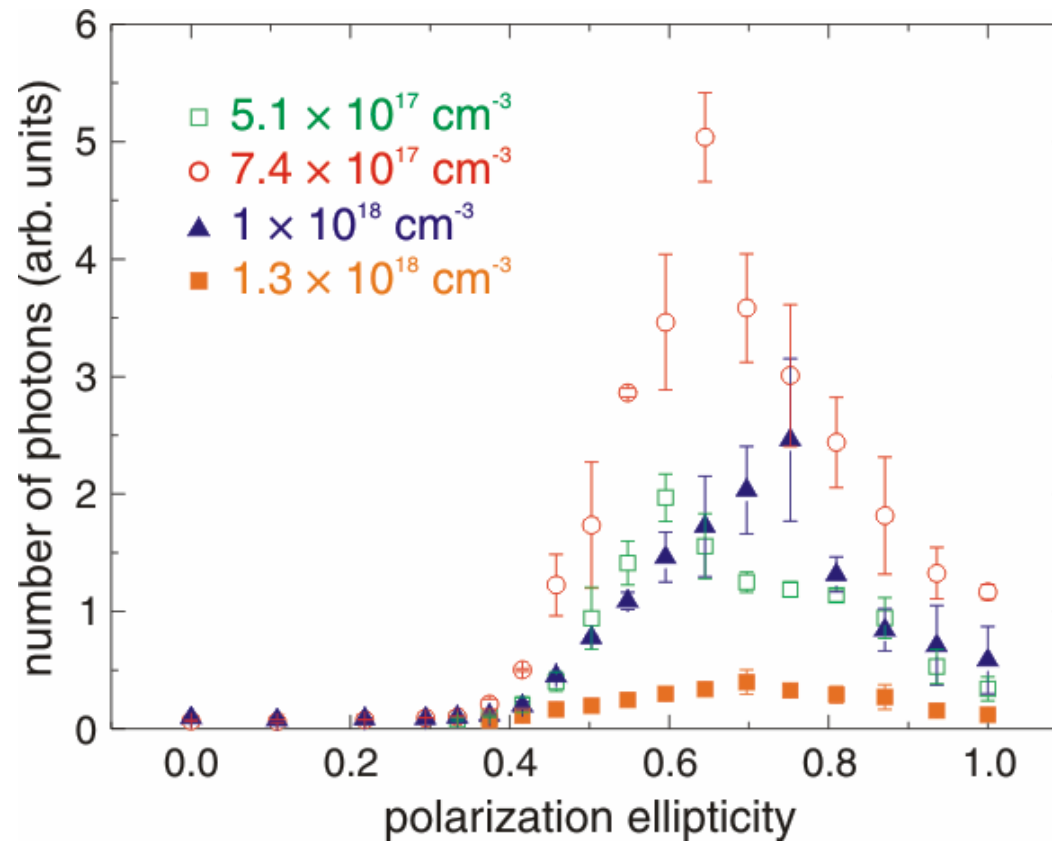
45 fs, 210 mJ, polarization ellipticity = 0.65
focus position at 2500 μm



- This reveals that the decreased lasing photon number at an atom density higher than the optimal value comes not only from the decrease of gain length and increase of length of absorption as a result of ionization-induced refraction, but also from a reduction of gain caused by, e.g., collisional de-excitation of the upper level.

X-ray lasing intensity vs. pump polarization ellipticity

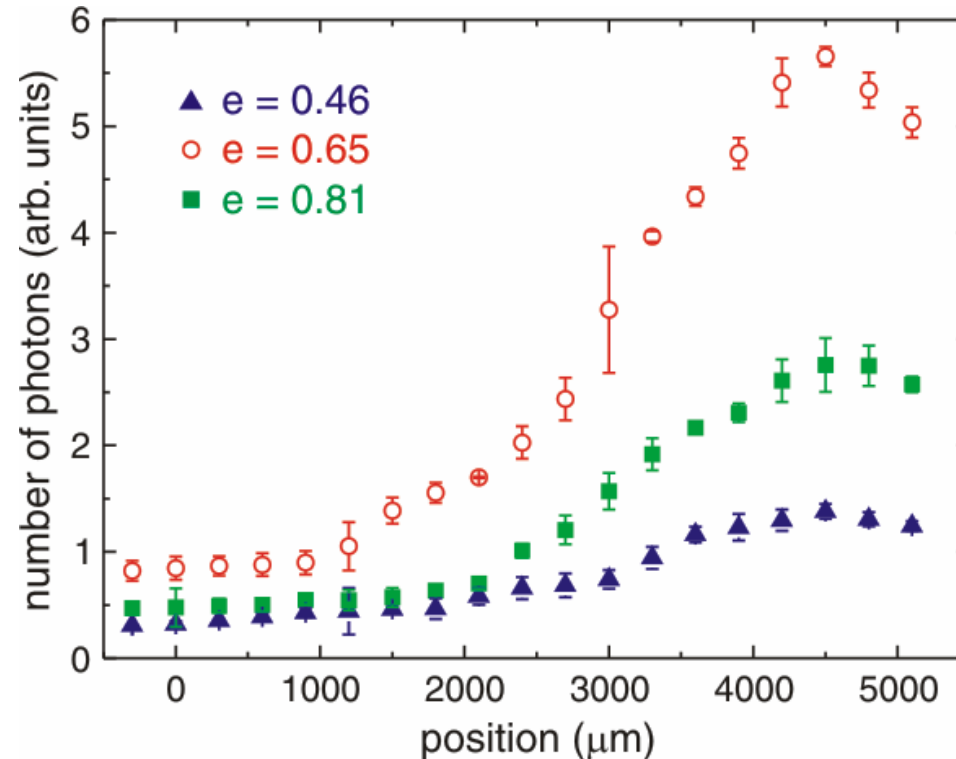
45 fs, 210 mJ, focus position at 2500 μm



- The presence of an optimal pump polarization ellipticity for maximum x-ray lasing at other than the circular polarization was observed.

Growth of x-ray intensity with pump propagation for various pump polarizations

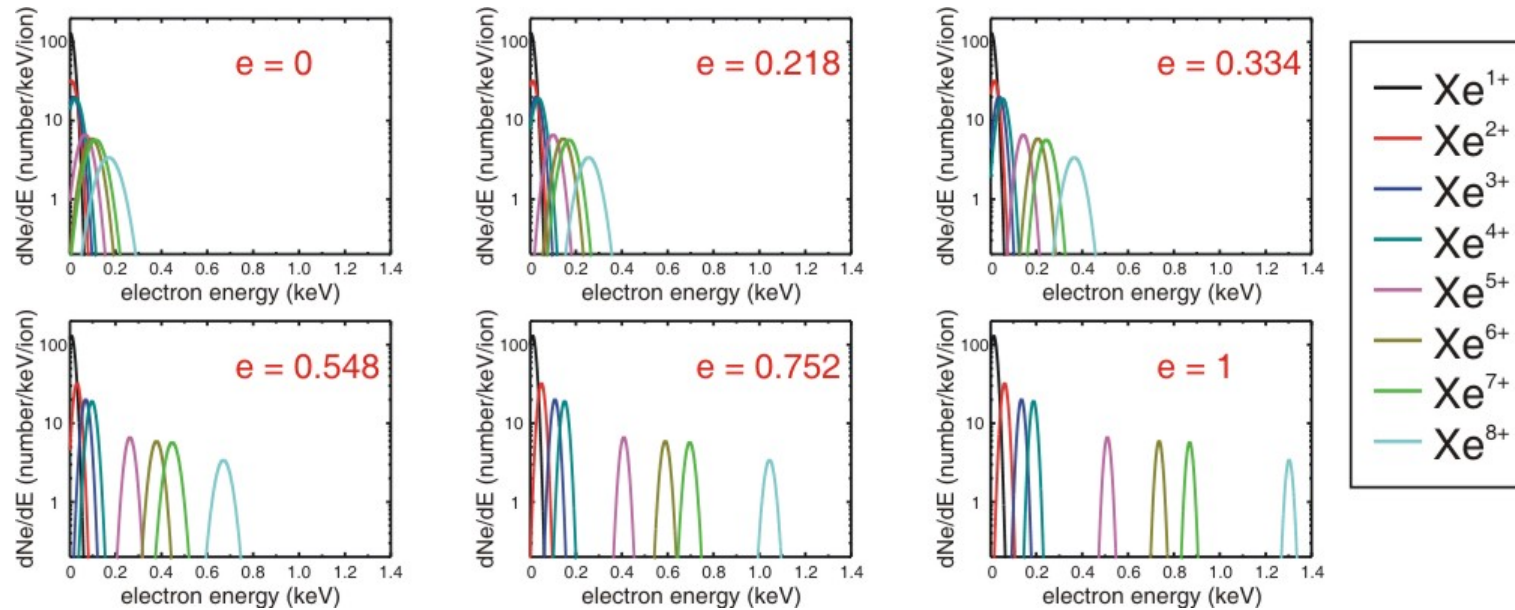
45 fs, 210 mJ, focus position at 2500 μm
atom density: $7.4 \times 10^{17} \text{ cm}^{-3}$



- The dependence of the small-signal gain on polarization ellipticity indicates that a mechanism that changes the electron energy spectrum from that produced by ATI heating is present and it results in a decreased collisional excitation rate when the polarization ellipticity is larger than the optimum.

Mechanism that leads to down-shift of the optimal pump ellipticity

electron energy spectrum for various polarizations



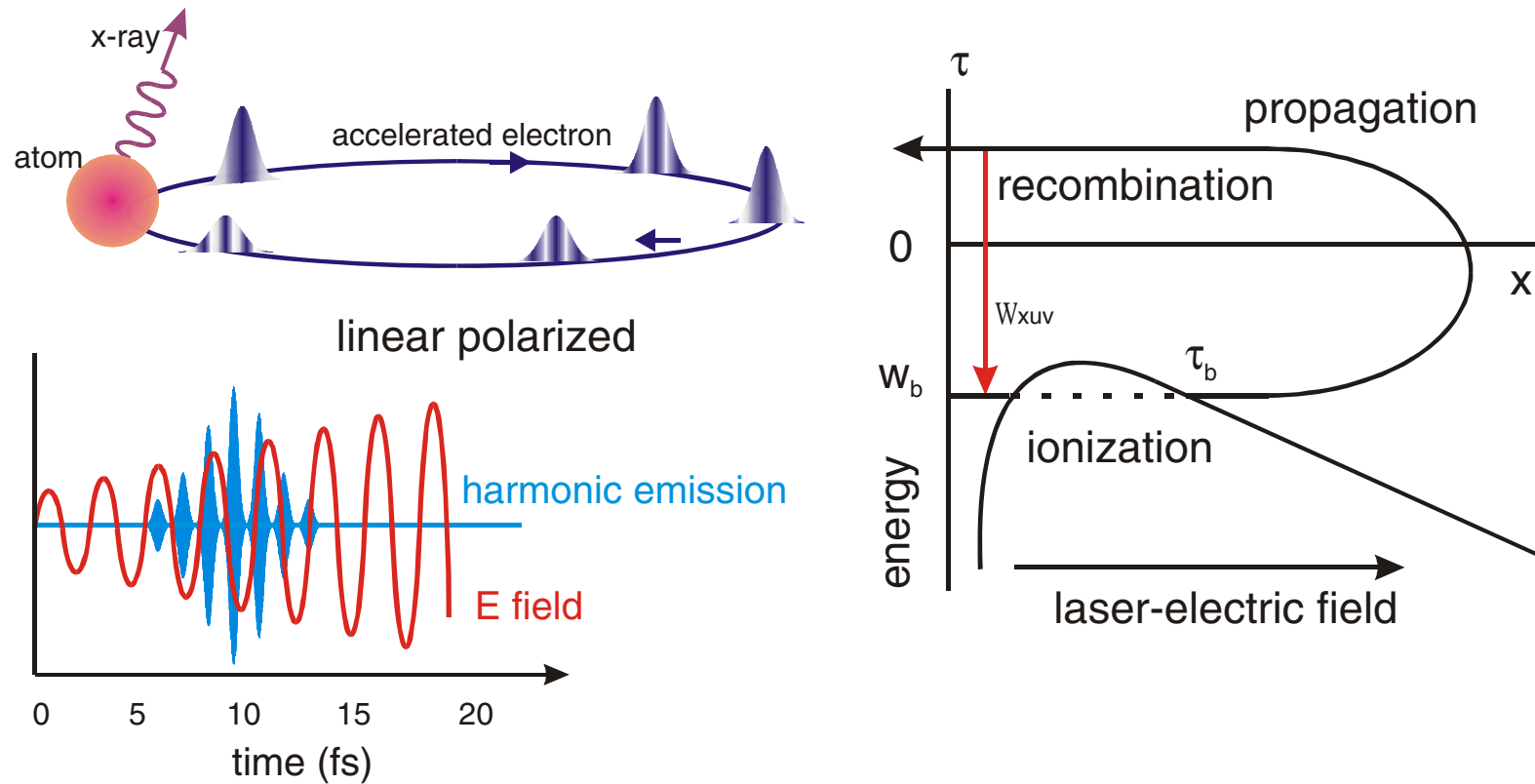
- The underlying mechanism is believed to be the laser-cluster interaction at the ionization front. If collisional heating and ionization during laser-cluster interaction can ionize Xe atoms to Xe³⁺ and Xe⁴⁺, then these pre-ionized electrons can not obtain the optimal energy for collisional excitation from the interaction of the pump pulse, greatly reducing the lasing intensity. By decreasing the polarization ellipticity the ATI energy of the electrons produced from higher ionization stages can be lowered to the optimal region and thus increases the gain.

Tomography of high-field physics in a gas jet

Tomography of high-harmonic generation in a gas or cluster
jet

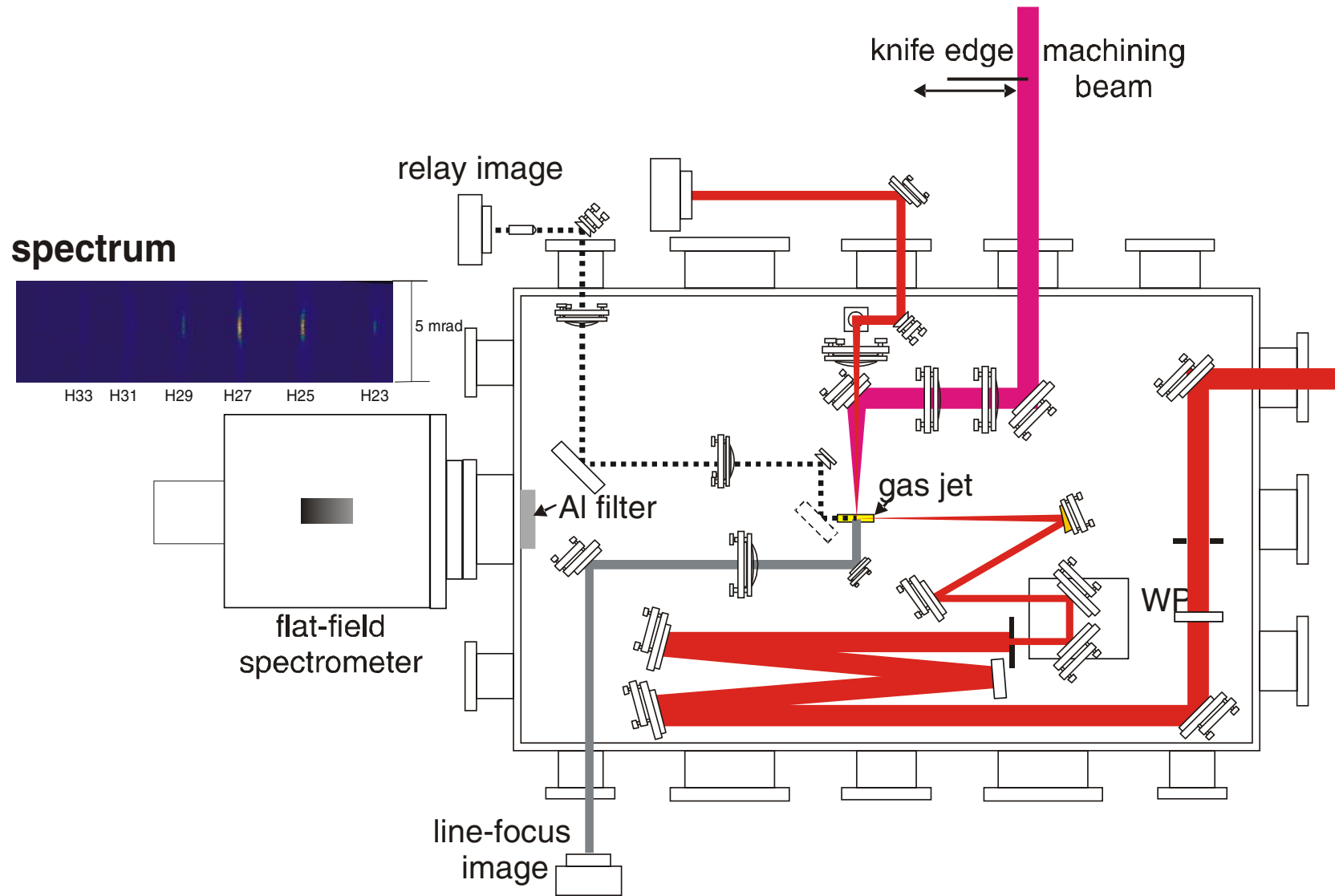
Optics Letters **31**, 984 (2006)

High harmonic generation from ionization and recollision of electrons

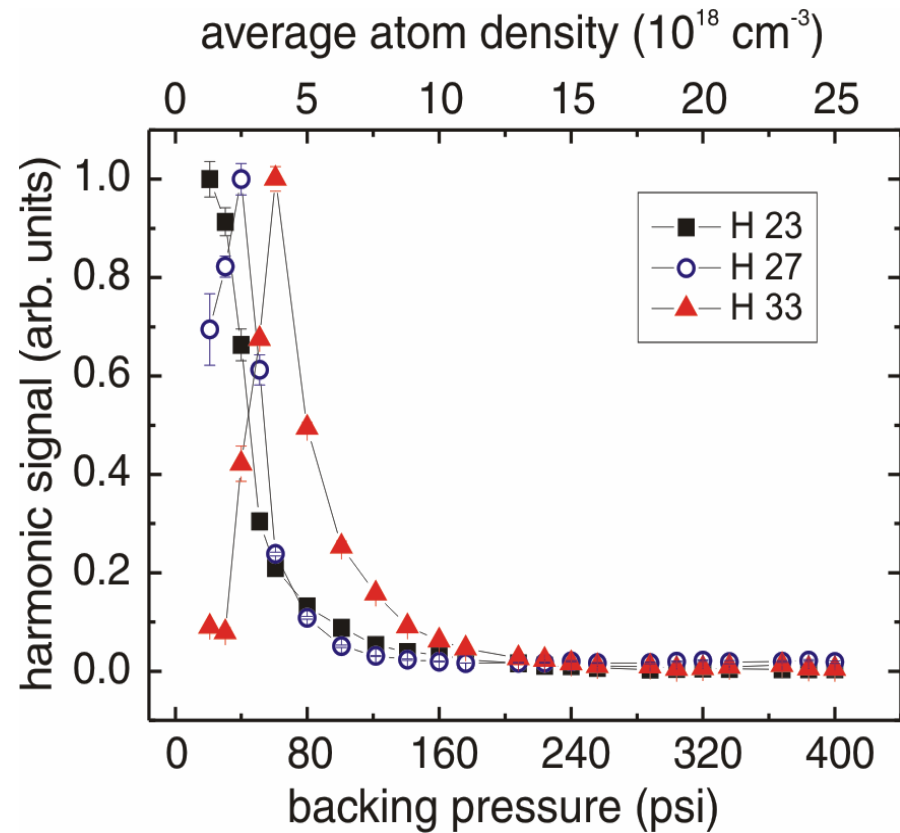


- The mechanism of harmonic generation is usually described by a three-step model: step 1, tunneling ionization; step 2, propagation and acceleration in laser electric field; step 3, radiative recombination.

Experimental setup

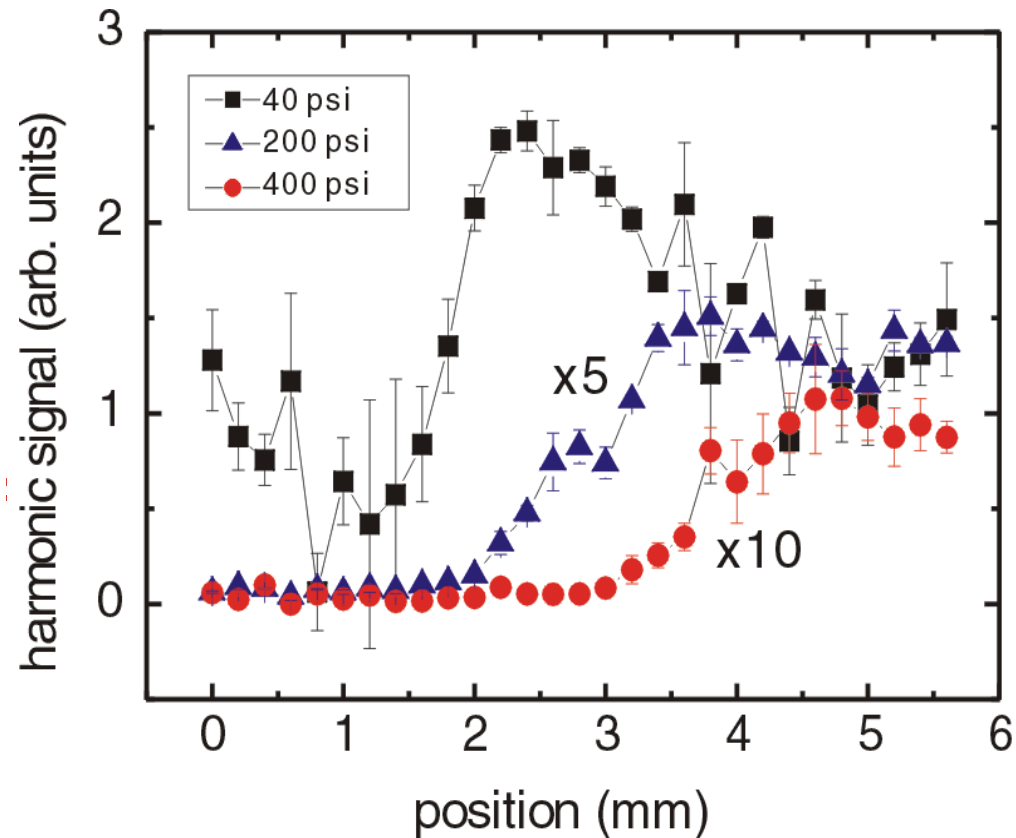


Intensities of harmonics vs. backing pressure



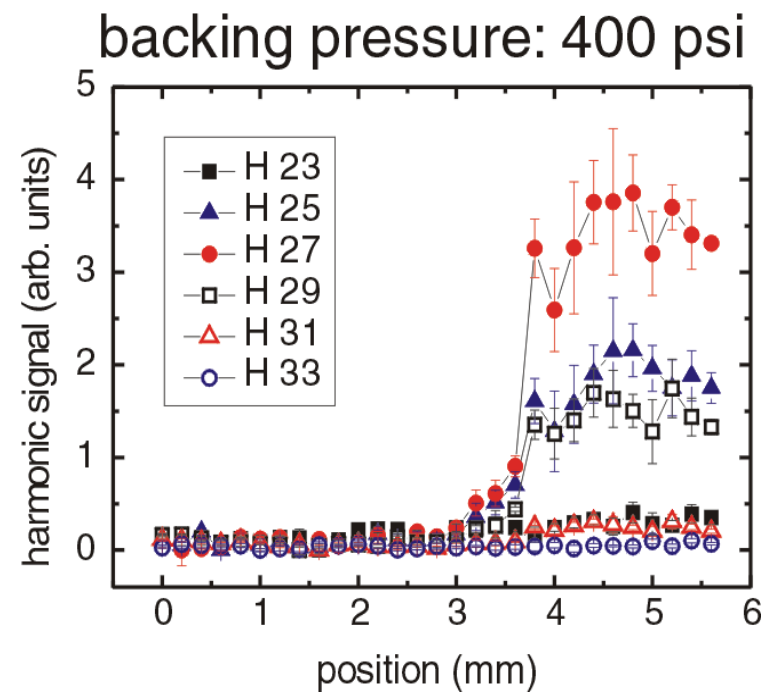
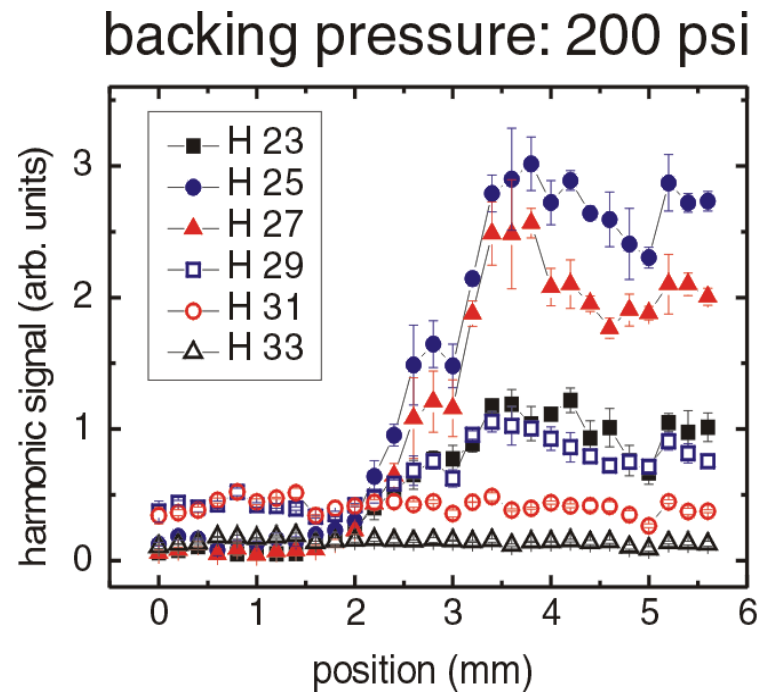
- There is an optimal gas-jet backing pressure for each harmonic order, which increases with higher harmonic order.

Growth of the 25th harmonic with laser beam propagation



- For higher backing pressure rapid growth of the 25th harmonic starts at a later position and the slope is smaller. Such a dependence of growth rate on backing pressure leads to the drop off of overall harmonic production for high backing pressures and thus the appearance of an optimal backing pressure.

Growth of various harmonics with laser beam propagation



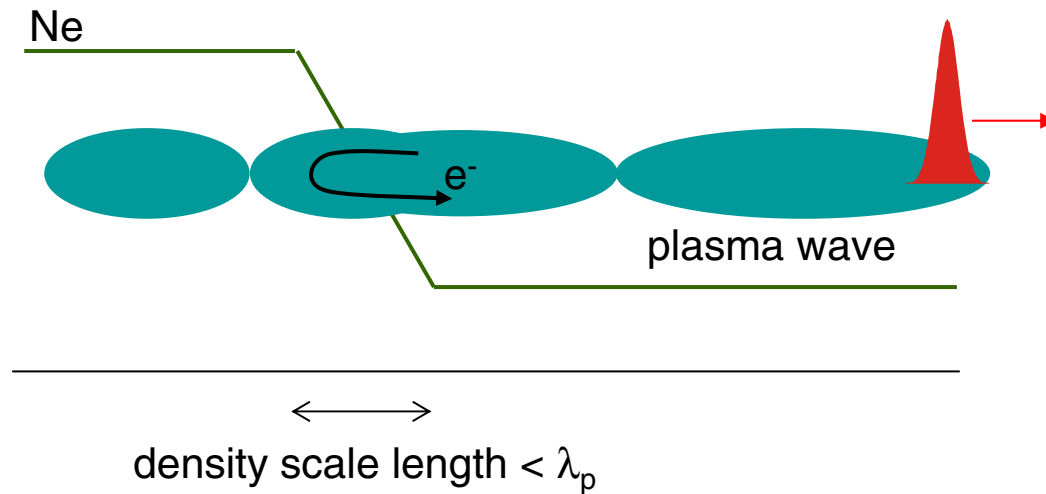
- At 200 psi and 400 psi backing pressure the regions of fast growth are similar for all of these harmonics. This indicates that the variations of the position of fast growth and saturation with respect to backing pressure is not due to larger x-ray reabsorption at higher backing pressure.
- Therefore, the dominant effect for the observed growth curves and the optimal backing pressure should be the phase-matching condition which may change significantly for different backing pressures as a result of varying cluster size.

High-field plasma devices

Electron injector

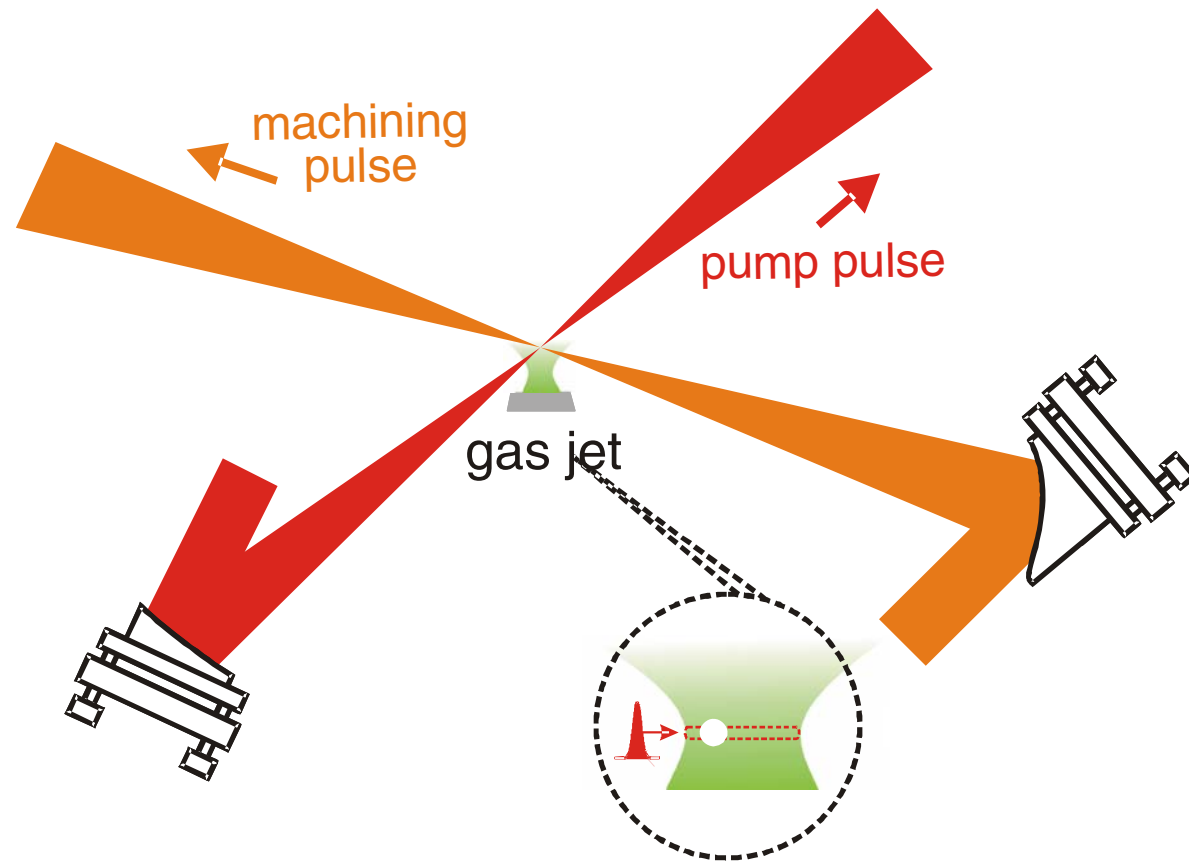
Physical Review Letters **94**, 115003 (2005)

Electron injection in a plasma wave by a sharp downward density ramp



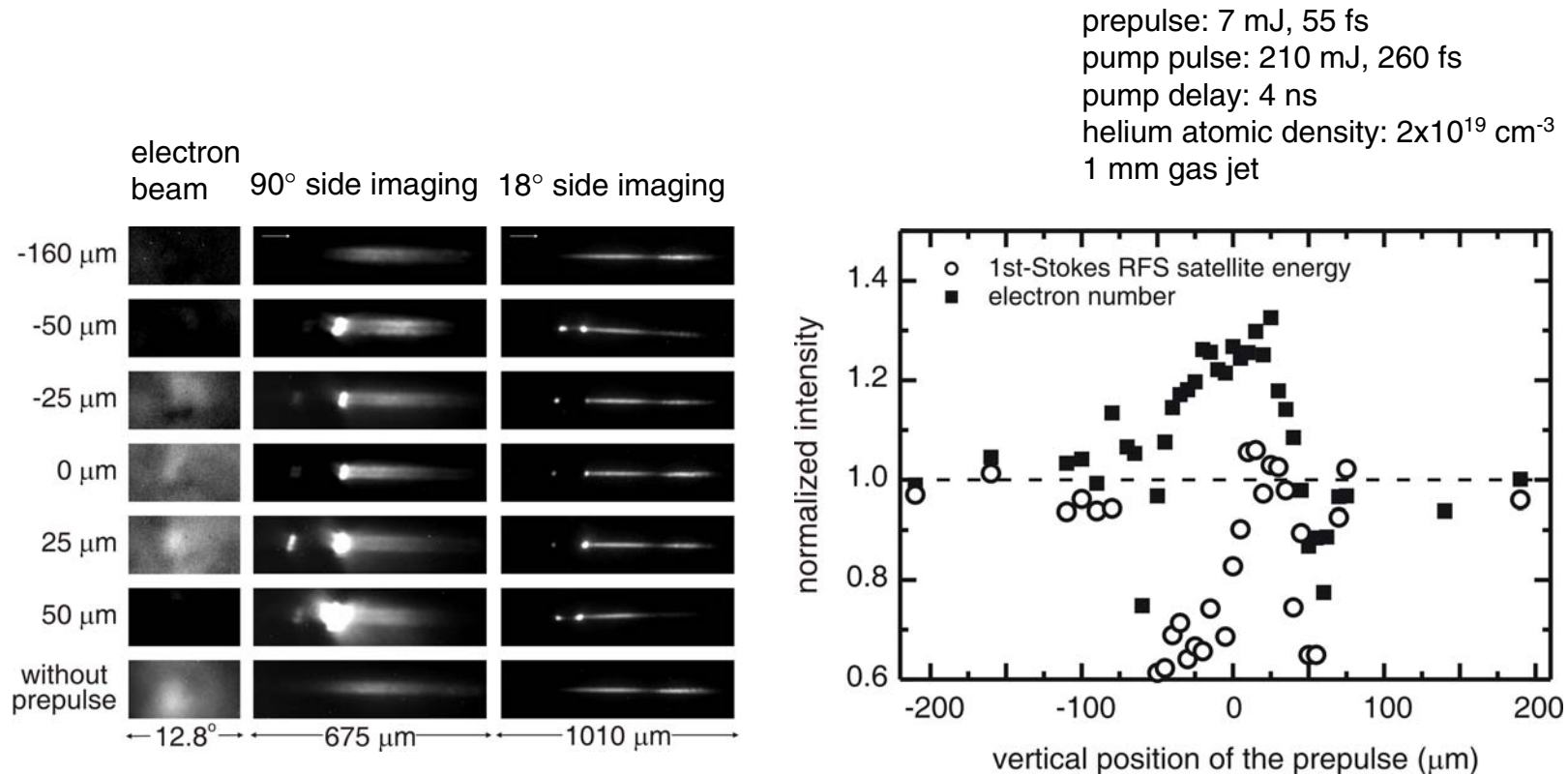
- When a plasma wave is generated across a sharp density down-ramp, electrons near the boundary moves toward the higher density region and then oscillate back into the lower density region. Since the oscillation period is longer in this region, these electrons are dephased with respect to the background plasma-wave electrons and thus become trapped. For significant self-injection to occur, the scale length of the ramp should be close to or less than the plasma-wave wavelength.

Experimental setup



- A sharp density transition can be produced by using another laser beam to drill a hole across the propagation path of the pump laser pulse.

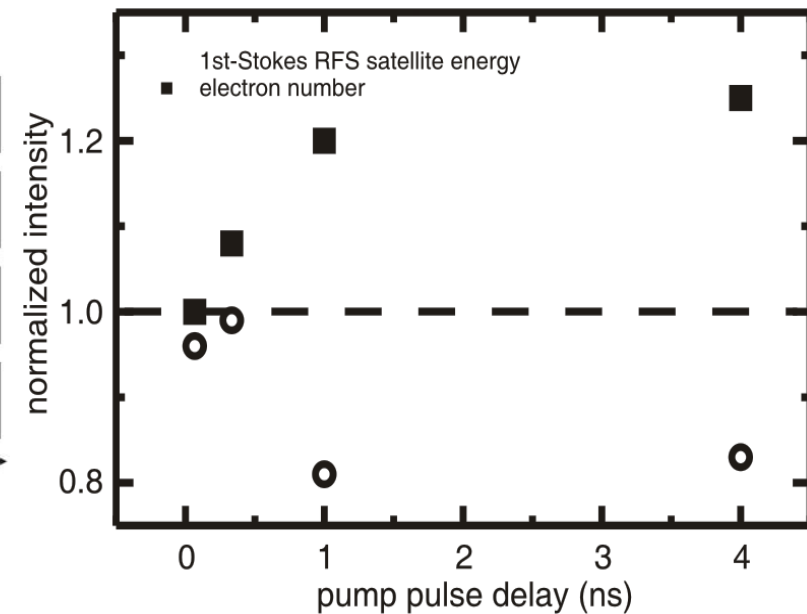
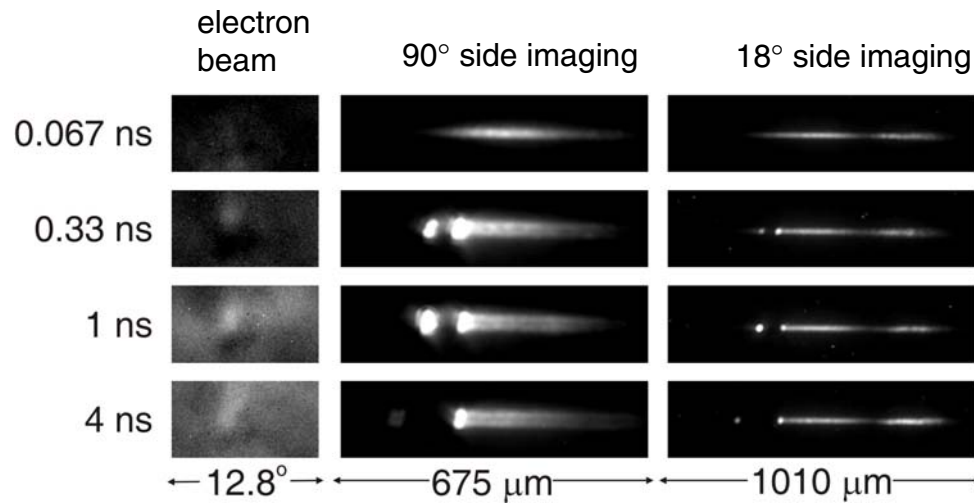
Raman intensity & electron number vs. vertical position of the density depression channel



- Additional injection of electrons is observed when the density depression channel intersects the propagation path of the pump pulse. Enhancement of self-trapping of electrons by enhanced RFS is ruled out since there is no increase of RFS intensity.

Raman intensity & electron number vs. pump pulse delay

prepulse: 7 mJ, 55 fs
pump pulse: 210 mJ, 260 fs
vertical position of the drilling pulse: 0 μm
helium atomic density: $2 \times 10^{19} \text{ cm}^{-3}$
1 mm gas jet

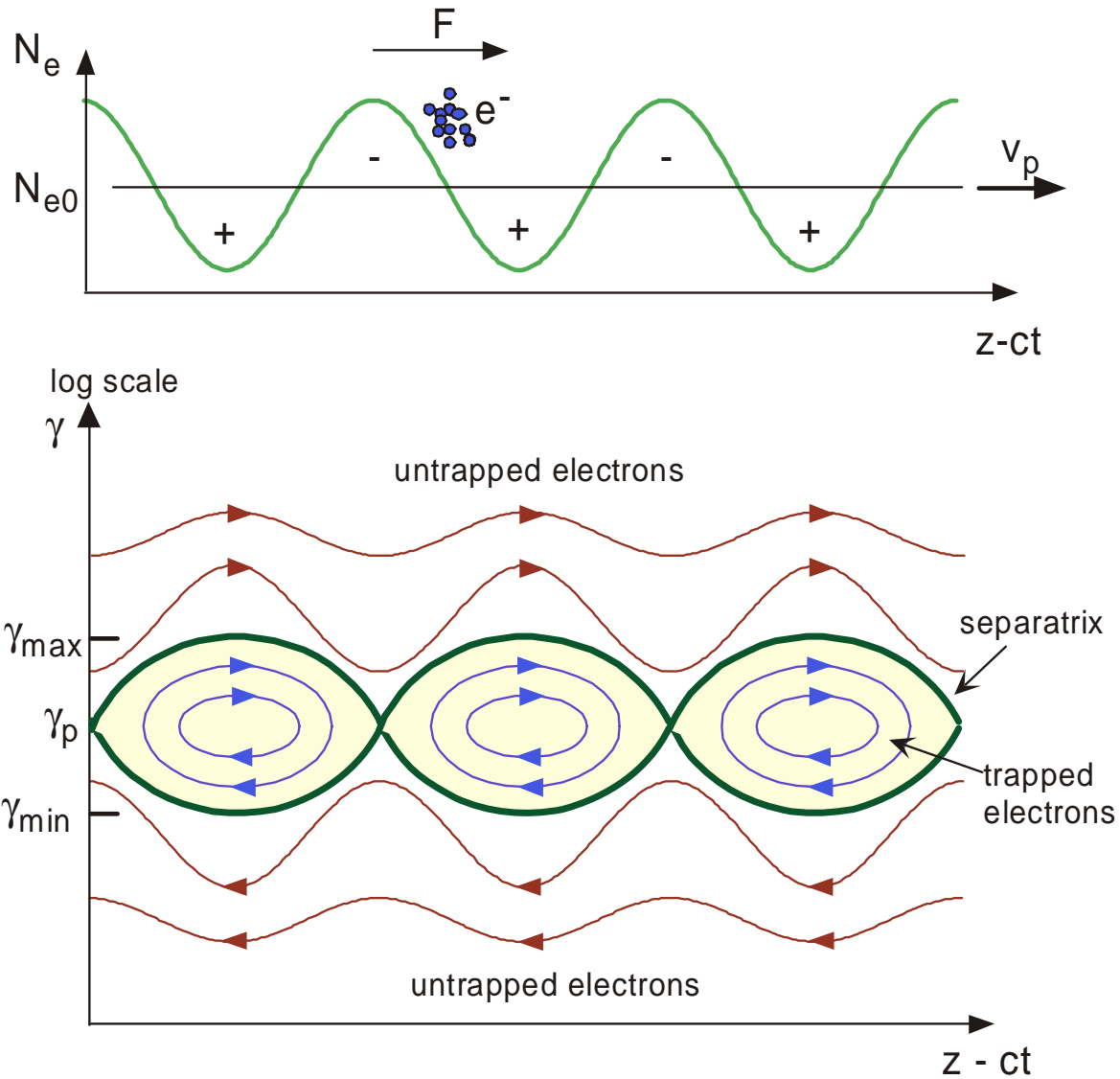


- The density ramp becomes sharper with the increase of pump-pulse delay, leading to increased number of self-injected electrons.

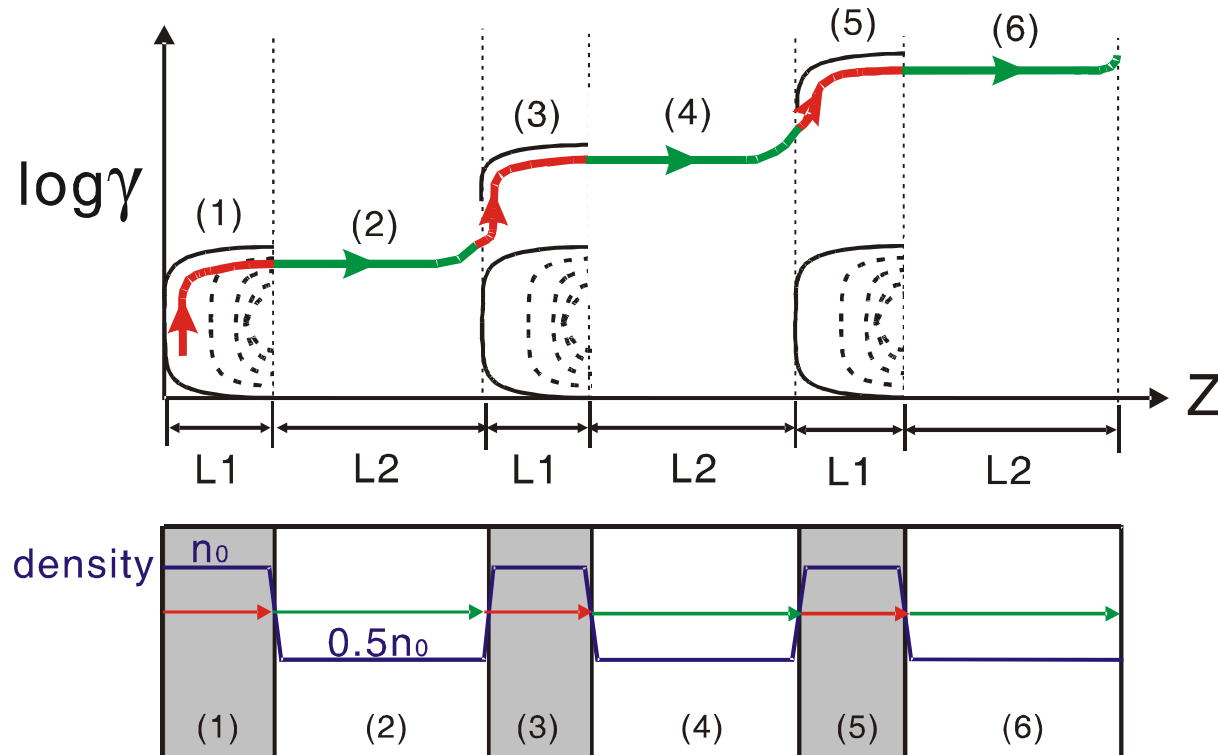
High-field plasma devices

Quasi-phase matching of harmonic generation and particle acceleration

Separatrix for electron motion in an electron plasma wave

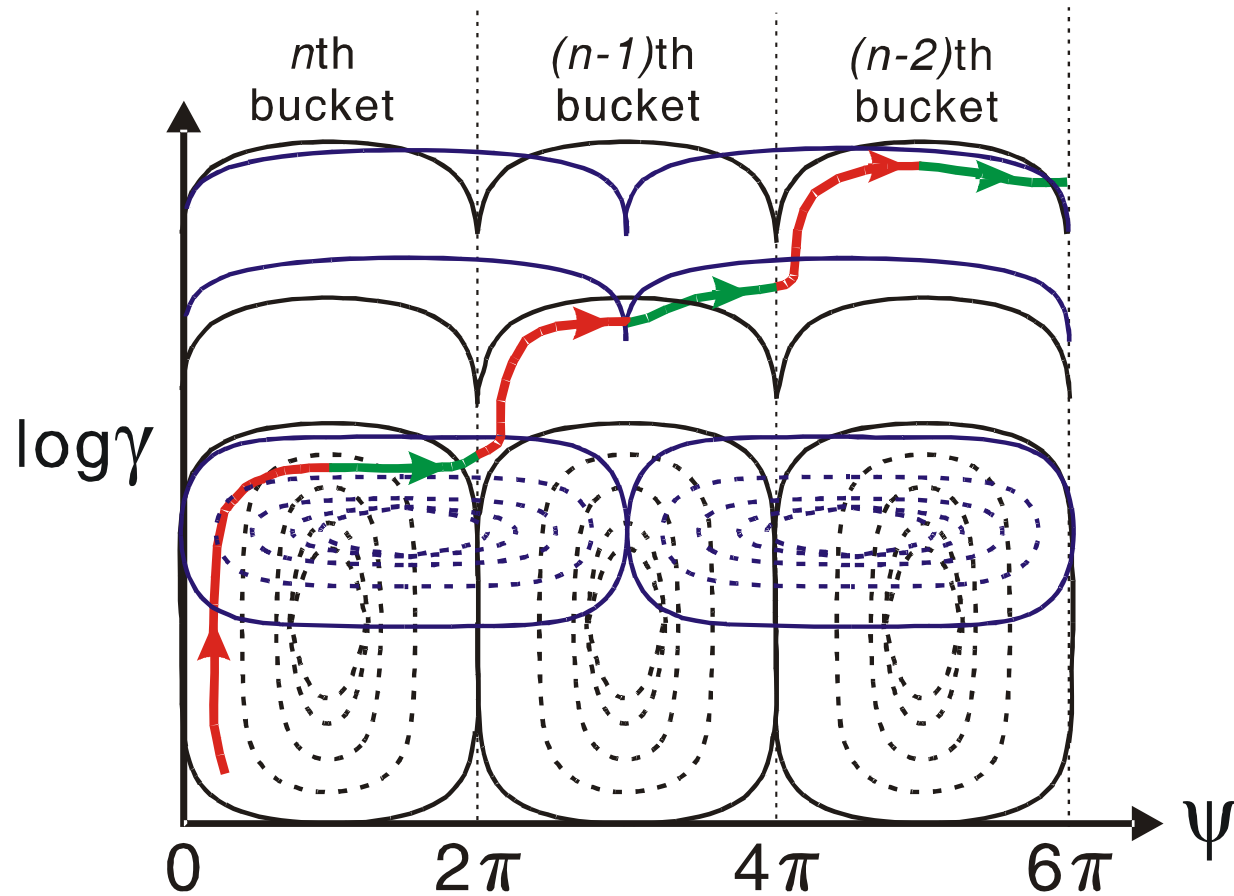


Evolution of energy of injected electrons with time in the lab frame



- By lowering the electron density in the deceleration sections along the pump propagation path and increasing their lengths accordingly, the accelerated electrons can be made to fall into the acceleration phase again when they reach the next high-density section.

Evolution of energy of injected electrons with time in the plasma-wave frame



- When the electron enters the next period of the density structure, in the moving frame of the plasma wave the electron enters the acceleration phase of the preceding bucket.

Obtain net energy gain in each period (stage)

Under the quasi-phase matching condition the net energy gain in each period becomes zero if the electric field in the plasma wave is linearly proportional to plasma density.

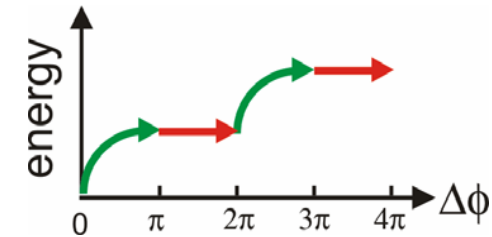
Such cancellation can be broken to obtain significant gain in each period (stage) by many ways.

- Relativistic self-guiding should result in a smaller beam size in the high-density sections and thus lead to a larger intensity for breaking the cancellation.
- The electron may gain or lose energy in the low-density sections and thus if many stages are implemented, the overall contribution from these low-density sections to energy loss may be averaged to zero.

Various schemes of quasi-phase matching

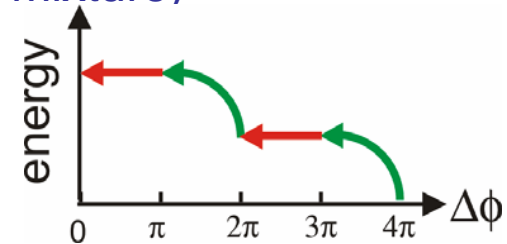
- electron acceleration in a plasma wave

➔ forward ladder climbing



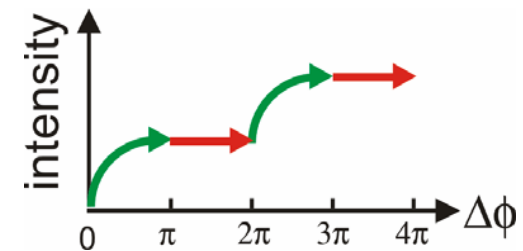
- proton acceleration in a plasma wave (Ar/H₂ mixture)

➔ backward ladder climbing



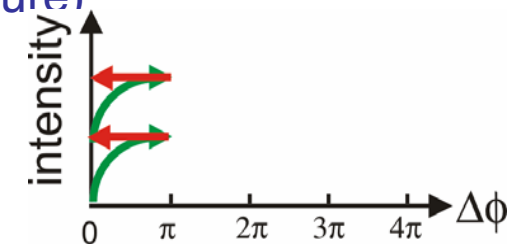
- harmonic generation in a plasma (H₂)

➔ forward ladder climbing



- harmonic generation in a plasma (Ar/H₂ mixture)

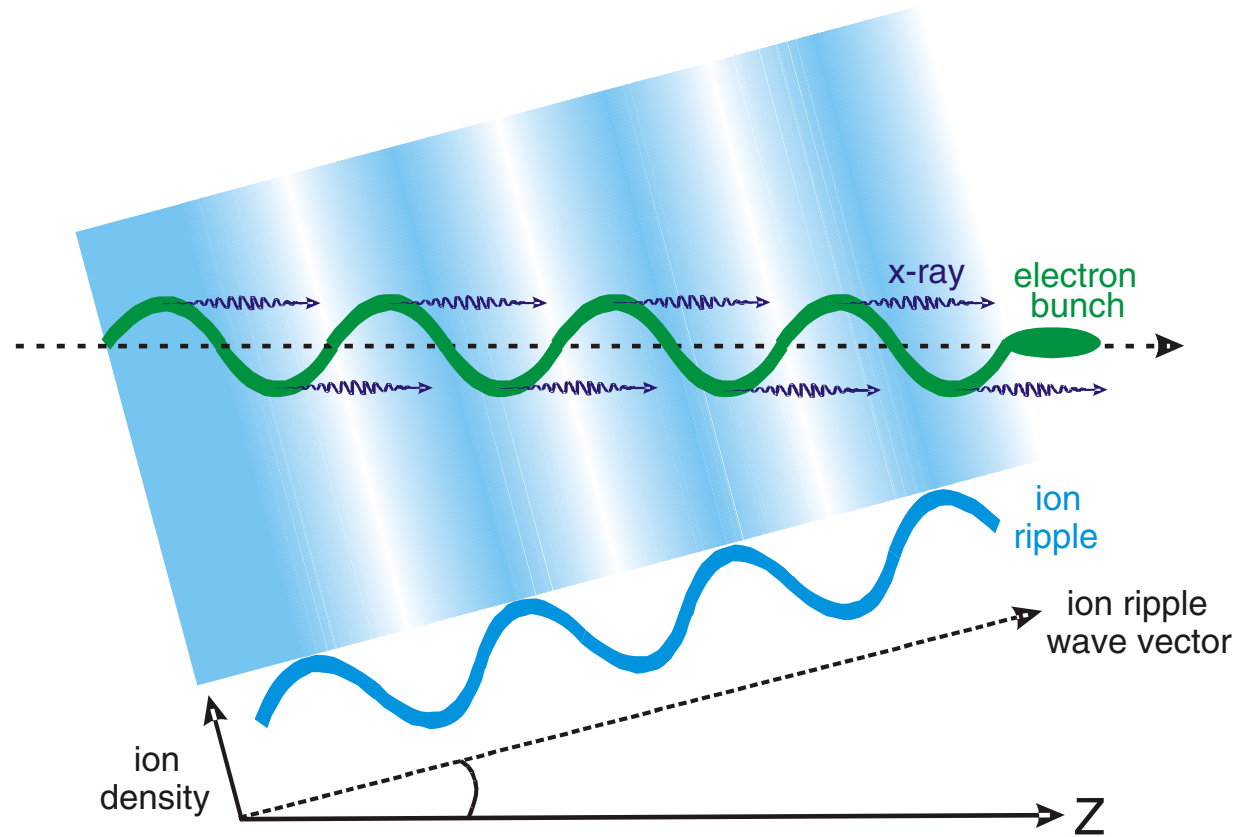
➔ vertical ladder climbing



High-field plasma devices

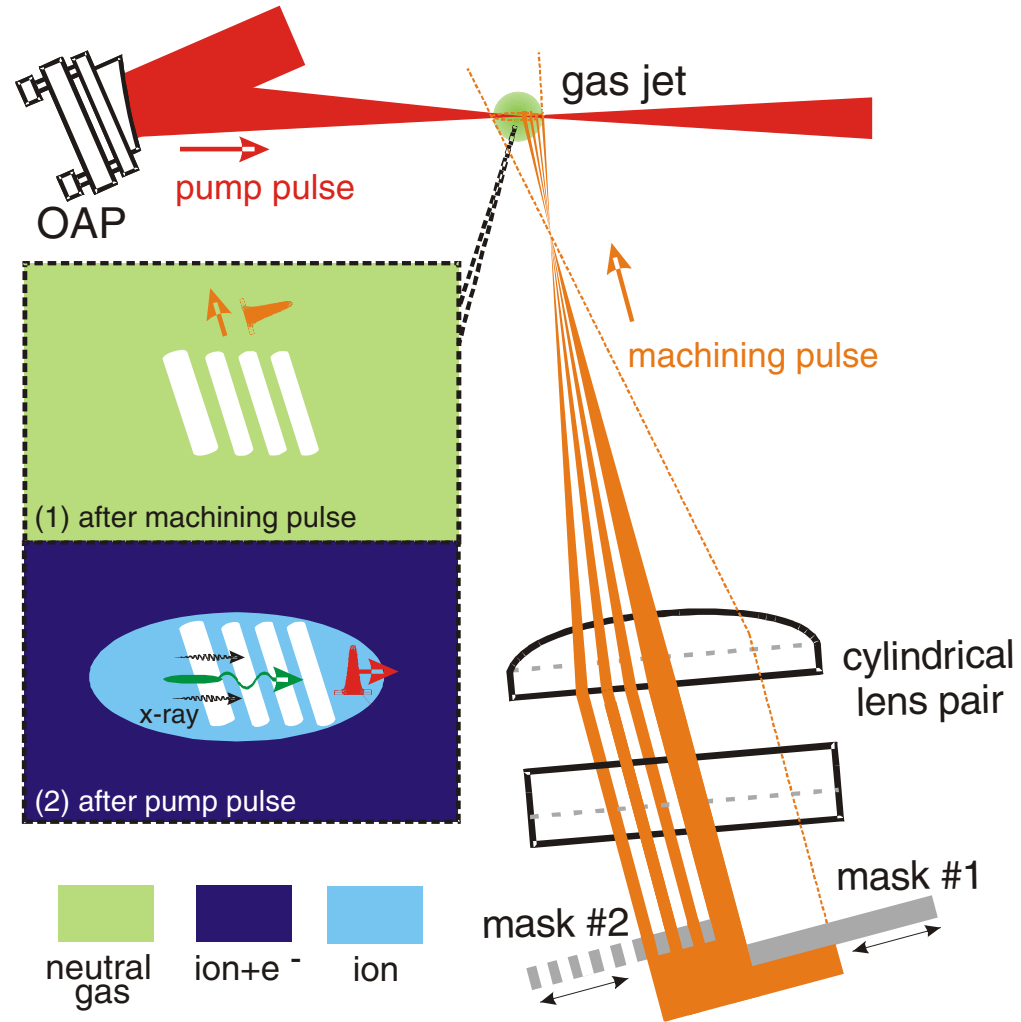
Electron wiggler for x-ray production

Ion ripple laser



K. R. Chen and J. M. Dawson, *Phys. Rev. Lett.* **68**, 29 (1992)

Experimental setup for producing the ion ripple



Conclusion

Conclusion

- The tomographic method can add a crucial dimension to the whole array of existing diagnostics for laser beam, plasma wave, electron beam, and x-ray beam, etc.

For examples, measurements of 3D profile of pump pulse propagation and spatio-temporal evolution of plasma wave may also be achieved.

With this method the details of the underlying physical processes in laser-plasma or laser-gas interaction can be observed and compared directly to the observations in simulations.

- In a way similar to the fabrication of semiconductor photonic devices, the capability of fabrication of density structures in a gas jet provides a whole array of elements of high-field plasma devices.

By integration of these elements, customized or adaptive devices for generating the desired products with great efficiency may be accomplished.

For instance, by integrating the electron injector, the quasi-phase-matched accelerator, and the wiggler, the entire architecture of a synchrotron radiation source may be constructed in a single gas jet.